TESI DOCTORAL

Autora: Amaya Virós Usandizaga

Títol: Mouse Models in the Study of Malignant Melanoma

Departament: Medicina

UNIVERSITAT AUTÒNOMA DE BARCELONA

Data: Febrer 2013

Thesis Title:

Mouse models in the study of malignant melanoma

Author:

Amaya Virós Usandizaga

Department of Medicine

Universitat Autonoma de Barcelona

February 2013

Directors:

Vicente García-Patos Briones

Richard Marais

Index

Acknowledgements

This work would not have been possible without the support of my two friends and codirectors Richard Marais and Vicente García-Patos. My utmost gratitude to both Vicente and Richard, I will never forget your high standards, your encouragement, support and inspiration.

Thank you to current and former colleagues in the Marais' Lab who have helped me through the journey and have generously shared time and ideas with me. My special thanks to those who have helped me overcome the hurdles a medic will invariably stumble upon in the lab. You have all been patient and kind and I am so blessed I learned from you. Malin Pedersen, Romina Girotti, Berta Sanchez-Laorden, and Grazia Saturno; I am in your debt. Special thank you to Carla Milagre and Joel Rae, my thesis wouldn't be as it is today without both of you. Thank you to Matthew Martin and Nathalie Dhomen for their good spirit and making our common work a pleasure. To Robert Hayward thank you for being brilliant and infinitely helpful and organized.

This work would not be possible without the invaluable help of our team leader collaborators and the members of their labs: in particular Jorge Reis-Filho and Caroline Springer, who both went beyond the call of duty to help me. Thank you to Roger Lo and his team, Dorothy Bennett and BJ Longley.

Thank you to my husband and children who expect the best and give me the strength to do my best.

Thank you to my loving parents for all they do and have done. This is a very long list of things, I am afraid, so I will summarize. You gave me love and a good education. What else could a child ever ask for?

Mouse models in the study of malignant melanoma

Summary:

We present three publications summarizing the investigations in mouse models of melanoma proposed as a subject for a doctoral thesis. In the first publication we present how oncogenic ^{V600E}BRAF expression in adult mouse melanocytes combined with KITL expression in mouse keratinocytes translocates melanocytes to the epidermis but does not lead to a more "humanized"form of melanoma. Tumours in this mouse model fail to replicate the cardinal features of ^{V600E}BRAF -driven human melanomas, where there is a prominent radial growth phase. Mice melanomas in the ^{V600E}BRAF-KITL model more closely resemble tumours induced in the ^{V600E}BRAF model without expression of KITL, where tumours are dermal, invasive, and present no radial growth phase. However, the ^{V600E}BRAF-KITL model translocates melanocytes to the epidermis and leads to the development of naevi of distinct phenotype. Importantly, coexpression of ^{V600E}BRAF and KITL leads to dermal melanomas that appear with a higher penetrance and shorter latency.

Our second study shows how the recently approved BRAF inhibitors for the targeted treatment of metastatic malignant melanoma driven by oncogenic BRAF lead to the appearance of squamous cell carcinoma (SCC) and keratoacanthoma in approximately 25% of patients. Using a mouse model of skin carcinogenesis leading to the formation of SCC in mice, we show how the addition of a BRAF inhibitor accelerates the course of disease. We hypothesized that *RAS* activation in keratinocytes might interact with RAF inhibitor therapy to promote cell proliferation, ultimately resulting in KAs and cSCCs. We show indirect evidence the mechanism underlying SCC development in the context of BRAF inhibitor treatment is the paradoxical activation of the MAP Kinase pathway in both humans and mice. While RAF inhibitors inhibit mitogen-activated protein kinase (MAPK) signaling in *BRAF*-mutant melanoma cells, they may also cause a paradoxical increase in MAPK signaling in the context of mutated or activated *RAS*. Our results strongly suggest *RAS* mutations in actinic keratoses, the premalignant skin lesions with the potential to transform into cSCC, are driven to proliferate when treatment with a BRAF inhibitor

is initiated. We show these lesions are highly proliferative in humans and in our mouse model, and respond to the FDA approved antiproliferative drug 5 Fluorouracil. Our mouse model also helps develop a new treatment rationale for metastatic melanoma with an underlying BRAF mutation. We show how downstream inhibition of the MAP Kinase pathway with a MEK inhibitor is able to abrogate the development of SCC.

Resumen:

Presentamos tres publicaciones que resumen la investigación de la propuesta doctoral en modelos de melanoma en ratón. En la primera publicación presentamos como la expresión del oncogén ^{V600E}BRAF en melanocitos de ratón adultos combinado con la expresión en queratinocitos adultos del mismo ratón de KITL logra traslocar los melanocitos de la dermis a la epidermis de los ratones. Sin embargo, la inclusión de melanocitos epidérmicos no logra generar un melanoma en el ratón que replique las características primordiales del melanoma en humanos. Los tumores en el ratón siguen siendo principalmente de ubicación dérmica, sin componente epidérmico, y no presenta una fase de crecimiento radial. Los tumores en el modelo ^{V600E}BRAF-KITL son muy invasivos y presentan destrucción local en la dermis, similares a los melanomas que surgen en el modelo ^{V600E}BRAF. Lo que si ocurre con el modelo de ratón ^{V600E}BRAF-KITL es que en la epidermis normal vemos el depósito de melanocitos en la epidermis interfolicular, algo no observado en ratones normales o ratones ^{V600E}BRAF. Igualmente, los nevus dérmicos que se forman tienen un fenotipo distinto, con mayor numero de células en la dermis papilar. Otro de los hallazgos importantes es que los melanomas que surgen en este modelo de ratón surgen en mayor numero (mayor penetrancia) y con una latencia más corta que los melanomas en el modelo tradicional ^{V600E}BRAF.

Nuestro segundo estudio investiga la aparición de los carcinomas escamosos y los queratoacantomas (cSCC y KA) que surgen en 25% de pacientes como efecto secundario a los nuevos fármacos inhibidores del oncogén BRAF. Estos fármacos se han demostrado eficaces en el tratamiento del melanoma maligno metastático, prolongando la supervivencia de pacientes. En nuestro estudio, utilizamos un modelo de ratón de carcinogénesis de escamosos cutáneos para demostrar como la utilización de inhibidores de BRAF es capaz de acelerar la progresión tumoral en estos pacientes. Nuestra hipótesis es que la activación del oncogén RAS en queratinocitos puede

interaccionar con inhibidores de BRAF para promover la proliferación celular, que llevaría al desarrollo de KA y cSCC en los pacientes. Nosotros demostramos evidencia indirecta que el mecanismo que subyace el desarrollo de tumores de estirpe queratinocítica en estos pacientes es la activación paradójica de la vía de proliferación celular MAP Kinase tanto en ratones como humanos. Los inhibidores de BRAF inhiben la vía MAP Kinase en células que portan una mutación BRAF, pero paradójicamente son capaces de inducir una activación de la misma vía en células que en lugar de mutación en BRAF tienen mutación en RAS.

Nuestros resultados sugieren que las mutaciones en queratosis actínicas (lesiones premalignas precursoras de KA y cSCC) proliferan cuando los pacientes inician tratamiento con inhibidores de BRAF para su melanoma metastático.

En nuestro tercer estudio demostramos como las lesiones inducidas por inhibidores de BRAF son altamente proliferativas y responden al antimetabolito 5-Fluorouracilo aprobado para el uso de lesiones queratinocíticas cutáneas premalignas. Nuestro modelo de ratón en este artículo nos permite desarrollar una nueva guía para el tratamiento de pacientes en estadios avanzados de melanoma metastático BRAF. Demostramos como la inhibición de MEK, una quinasa que señaliza en las últimas fases de activación de la vía MAP Kinase, es capaz de evitar el desarrollo de lesiones cutáneas, evitando la activación paradójica de MAP Kinase.

Introduction:

Melanoma is a potentially deadly form of skin cancer. Each year in Europe there are between 12 and 19 new cases of melanoma per 100,000 population. Melanoma rates continue to increase in most European countries, and in many of these countries, the rate is almost doubling every decade, disproportionately affecting younger people and leading to a significant loss in life-years in those affected[1]. Recent insights into the molecular mechanisms driving melanoma have revealed that the MAP Kinase pathway, signaling via RAS/RAF/MEK/ERK, plays a central role in melanoma development and maintenance. RAS is a small G-protein that is activated downstream of receptor tyrosine kinases (RTKs) and RAF, MEK and ERK are protein kinases that form a three-tiered cascade that controls cell growth and survival[2]. Gene re-sequencing campaigns of the three *RAS* genes (*HRAS*, *KRAS*, *NRAS*) and three *RAF* genes (*ARAF*, *BRAF*, *CRAF*) in humans have revealed that *NRAS* is

mutated in about 20% of melanomas and *BRAF* in a further 45% of cases[3]. In addition, mutations in the RTK *KIT* have been identified in 15-20% of acral and mucosal melanomas and large number of the other components from this pathway and from pathways that interact with this pathway are mutated at a lower rate in melanoma samples[4, 5].

The identification of the oncogenic drivers of melanoma has led to the development of new treatment strategies for this disease [6]. Drugs that inhibit BRAF such as vemurafenib and dabrafenib, or drugs that inhibit MEK, such as trametinib, can achieve improved progression-free and overall survival in ~80% of melanoma patients who suffer from BRAF mutant melanoma [7-10]. The FDA (US Food and Drug Administration) and EMA (European Medicines Agency) approved vemurafenib for use in BRAF mutant melanoma patients in 2011. It is likely that dabrafenib and trametinib will receive approval in the near future. The potential for targeted therapy in melanoma has been further exemplified by the clinical responses of KIT mutant melanomas to KIT inhibitors [11, 12]. Taken together, these data establish that the genetically distinct forms of melanoma must be treated with different drugs and must have different *in vivo* systems to study biology of disease and biology of response to treatments. Together with immunotherapies, which have also recently been shown to achieve impressive clinical responses in melanoma patients[13-15], the targeted agents represent a paradigm shift in the clinical management of melanoma by providing viable and effective treatments for this disease for the first time in three decades. It is unclear which genetic subtypes will benefit the most from immunotherapy, or combinations of both targeted and immunotherapy. There is a clear need to develop adequate tools to study the different subtypes of disease and therapeutics of response to new agents.

Notably, although the clinical responses of BRAF mutant melanoma patients to BRAF inhibitors are impressive, the majority of patients relapse after a relatively short period (6-8 months) of disease control [16, 17]. Importantly about 25% of patients who take vemurafenib present with rapidly developing multiple squamous cell carcinomas (SCC) in the first weeks of treatment. BRAF inhibitors such as vemurafenib block MAP Kinase signaling and cell proliferation in BRAF mutant melanoma cells, but in cells that express upstream oncogenic or activated RAS, they

promote the opposite effect and lead to an unexpected paradoxical activation of the pathway and cell proliferation. This is because inhibition of wild type BRAF in the presence of oncogenic RAS drives RAF proteins into a complex at the plasma membrane. This enables CRAF, a protein closely related to BRAF, to signal constitutively and hyperactivate the MAPK pathway[18, 19].

We hypothesized SCC in vemurafenib treated patients could be linked to the paradoxical activation of MAP Kinase pathway we see in the presence of RAS mutations. There is a scarcity of *in vivo* tools that aim to understand therapeutic responses to new, targeted drugs in melanoma. We also hypothesized judging from rapid growth observed in clinical cases of patients developing SCC after treatment with a BRAF inhibitor, these lesions would be highly proliferative and amenable to treatment with antiproliferative drugs such as 5 Fluorouracil (5FU). 5FU is approved for the use of squamoproliferative lesions such as actinic keratosis and Bowen's disease.

Recent work has aimed to develop mouse models of melanoma driven by oncogenic Braf that can emulate the more prevalent form of human melanoma. In humans, melanomas with a BRAF mutation tend to occur in younger individuals who have a prior history of intermittent sun exposure[3]. These melanomas are likely to appear at sites that have been intermittently sun exposed and are more frequent in patients with fair skin or who harbour genetic variants of the MC1R gene, which codes for red hair, freckles and blue eyes[20]. Melanomas with a BRAF mutation are also more likely to present specific histopathological criteria such as upward scatter of melanocytes and prominent pigmentation and nesting of the radial growth phase[21]. A recent mouse model of melanoma specifically mimics the acquisition of somatic *BRAF* mutations that occurs in human melanoma by expressing $Braf^{V600E}$ in the melanocytes of postnatal mice using the endogenous *Braf* gene. Expression of $Braf^{V600E}$ at physiological levels in adult mice leads to melanoma and proves mutated BRAF is a founder mutation in melanoma[22]. In mice, melanoma is largely restricted to the dermal layers of the skin and the epidermis is rarely involved. This difference presumably occurs because mouse melanocytes are predominantly located in the follicles and dermis and provide coat pigmentation, whereas human melanocytes are predominantly epidermal and provide protection from UV light.

Because mice do not present with interfollicular epidermal melanocytes, tumours in this model arise in the dermis and do not replicate de cardinal features of human melanoma driven by BRAF.

Melanocyte location in the skin is controlled by the KIT Lignad. Human keratinocytes express KITL throughout life and melanocytes therefore persist in the epidermis. In the postnatal mice, KITL expression is exclusively restricted to the hair matrix and the melanocytes are therefore mostly located in the hair follicle. When mouse keratinocytes are engineered to express KITL under the Keratin-14 gene promoter (K14), a proportion of melanocytes is able to remain in the epidermis well into adulthood **REF**.

We hypothesized expression of KITL in mouse keratinocytes and expression of ^{V600E}BRAF would lead to development of melanomas in mouse with a radial growth phase, which would more closely mimic human disease.

The aim of our work and doctoral thesis was to use mouse models of melanoma to investigate genetic events that lead to melanomagenesis and that can be used to investigate biology of response to new targeted therapies. Our work using mouse models of cancer has led to an increase in the knowledge of melanoma biology, as well as to a greater understanding of melanoma response to targeted therapies and side effects. This is manifested in the publications presented:

Publications:

1. (V600E)Braf::Tyr-CreERT2::K14-Kitl mice do not develop superficial spreading-like melanoma: keratinocyte Kit ligand is insufficient to "translocate" (V600E)Braf-driven melanoma to the epidermis. Rae J, **Viros A**, Hayward R, Bennett DC, Dhomen N, Longley BJ, Reis-Filho JS, Marais R. J Invest Dermatol. 2012 Feb;132(2):488-91.

2. RAS mutations in cutaneous squamous-cell carcinomas in patients treated with BRAF inhibitors. Su F*, **Viros A***, Milagre C*, Trunzer K, Bollag G, Spleiss O, Reis-Filho JS, Kong X, Koya RC, Flaherty KT, Chapman PB, Kim MJ, Hayward R, Martin M, Yang H, Wang Q, Hilton H, Hang JS, Noe J,

Lambros M, Geyer F, Dhomen N, Niculescu-Duvaz I, Zambon A, Niculescu-Duvaz D, Preece N, Robert L, Otte NJ, Mok S, Kee D, Ma Y, Zhang C, Habets G, Burton EA, Wong B, Nguyen H, Kockx M, Andries L, Lestini B, Nolop KB, Lee RJ, Joe AK, Troy JL, Gonzalez R, Hutson TE, Puzanov I, Chmielowski B, Springer CJ, McArthur GA, Sosman JA, Lo RS, Ribas A, Marais R. N Engl J Med. 2012 Jan 19;366(3):207-15. (*contributed equally)

3. Topical 5-Fluorouracil Elicits Regressions of BRAF Inhibitor-Induced Cutaneous Squamous Cell Carcinoma. **Viros A**, Hayward R, Martin M, Yashar S, Yu CC, Sanchez-Laorden B, Zambon A, Niculescu-Duvaz D, Springer C, Lo RS, Marais R.
   J Invest Dermatol. 2012 Aug 16.

Aims and methods:

Aim 1: To discover whether mouse models of melanoma described in the past could be altered to recapitulate the cardinal features of human melanomas; i.e, to combine genetic alterations in mice which may be able to transpose dermal mouse melanocytes to the epidermis and thus initiate epidermal melanoma with a radial growth phase. Because mice do not have epidermal melanocytes, when they are genetically engineered to develop melanoma they primarily develop dermal melanoma, which is thought to arise from follicular or dermal melanocytes.

Methods for Aim 1:
We developed a ^{V600E}BRAF-driven mouse melanoma model using tamoxifen-activated Cre-recombinase/loxP technology to express ^{V600E}BRAF-driven naevi and melanomas, which are known to be exclusively dermal. We tested if a membrane-bound KITL under the control of the K14 promoter is able to translocate these tumours to the epidermis.

Aim 2: To test whether mouse models may be useful in the field of melanoma to investigate *in vivo* biology of patient response to new molecular targeted therapy.

Methods for Aim 2:

Because oncogenic BRAF inhibitors block the active conformation of the BRAF kinase and patients present a better outcome as well as develop in 20-30% of cases well-differentiated cutaneous squamous cell carcinomas (cuSCC) and keratoacanthomas (KA), we used mouse models to investigate whether these lesions are driven by an underlying RAS mutation due to the paradoxical activation of MAP Kinase pathway in RAS mutant keratinocytes and disease progression in these cells, combined with a shut down of MAP Kinase pathway in melanoma cells with a BRAF mutation and no underlying RAS mutation.

We analysed whether squamoproliferative lesions arising in a human cohort of vemurafenib-treated patients harbour RAS mutations at a higher frequency than described in spontaneously arising KAs and cuSCC, which would drive MAPK pathway activation and rapid proliferation secondary to BRAF inhibition.

We used the two-stage skin carcinogenesis model, which activates *HRAS Q61L* mutations in mouse keratinocytes. Mouse skin is treated with the carcinogenic 7,12-dimethylbenz-(a)anthracene (DMBA) which then leads to tumour promotion in keratinocytes following application of 12-*O*-tetradecanoyl-phorbol-13-acetate (TPA). This system is known to then induce SCC in mice that are driven by ^{Q61L}*Hras* mutations. In our experiments, we treated mice with DMBA, TPA and the BRAF inhibitor PLX4720, a close analogue compound of vemurafenib, to see whether lesions suffered an acceleration of tumour formation and a shorter tumour latency when compared to the DMBA, TPA treated animals.

We also investigated whether ^{Q61L}*Hras* and *Hras* keratinoyctes, like RAS-driven melanoma cells, increase their proliferation and MAPK pathway activation secondary to BRAF:CRAF heterodimer formation following treatment with PLX4720. We investigated whether addition of a downstream MAP Kinase pathway inhibitor would abrogate the development of SCC in our mice.

Aim 3: To test whether SCC lesions developing rapidly in our mouse model of carcinogenesis under DMBA, TPA and PLX4720 treatment proliferate more rapidly and are responsive to treatment with the antiproliferative 5-Fluorouracil.

Methods for Aim 3:

We used the two-stage skin carcinogenesis model to analyse whether lesions arising in DMBA/TPA and PLX4720 treated mice had a high proliferation index in keeping with their rapid clinical course. We used Ki67 staining to assess proliferative index. We applied topical 5-Fluorouracil to individual lesions to investigate whether this could be a valid therapeutic alternative in SCC arising in vemurafenib treated patients.

We tested the use of 5FU in patients with eruptive squamoproliferative lesions consistent with early SCC and KA in two patients who developed multiple lesions following initiation of treatment with the BRAF inhibitor dabrafenib.

Results and discussion:

Our first aim experiments show how in mice where we combine the ^{V600E}BRAF-KITL genetic aberrations we are not able to develop melanoma that sufficiently replicates the cardinal features of human melanoma; there is no radial growth phase and only few epidermal melanocytes are visible under the microscope and with S100 specific stainings. The combined genetic targeting accelerates melanoma formation (shorter latency) and is more successful at driving the appearance and the number of dermal melanomas than the ^{V600E}BRAF model alone (higher penetrance). This combination induces higher numbers and size of intradermal nevi, and may be a valid mouse model for the *in vivo* study of naevi as well as of an accelerated ^{V600E}BRAF model. The melanomas in the ^{V600E}BRAF-KITL model we examined histologically are similar to tumours in the ^{V600E}BRAF model, where lesions are described as being poorly defined, asymmetric, ulcerated, and locally destructive. Cell morphology in both models is predominantly spindle, occasionally becoming a storiform pattern, with abundant mitoses.

Macroscopically, ^{V600E}BRAF-KITL mouse skin hyperpigmentation was enhanced compared to the ^{V600E}BRAF mouse. Microscopically, we showed there were melanocytes in the interfollicular epidermis and melanin capping of the nuclei in the keratinocytes. The naevi induced in the ^{V600E}BRAF-KITL model were more cellular, dermal tumours with large populations of heavily pigmented epitheliod and dendritic melanocytes which occasionally formed ill-defined nests, separated from the epidermis by a narrow Grenz zone. These naevi contrast with the naevi found in the ^{V600E}BRAF model, which are paucicellular and more dendritic, and predominantly located in the deep reticular and periadnexal dermis.

The results of our second and third aim show how *RAS* mutations are present in approximately 60% of cases in patients on vemurafenib for metastatic malignant melanoma, suggesting that preexisting, preclinical mutations of RAS in keratinocytes may confer a predisposition to the development of SCC. This is in stark contrast to the prevalence of RAS mutations in spontaneously arising SCC and KA, which is reported at 3-30%.

In the skin carcinogenesis model, the BRAF inhibitor PLX4720 induced the paradoxical activation of the MAPK pathway and proliferation of *HRAS Q61L*-transformed keratinocytes, with decreased latency and accelerated growth of cutaneous squamous-cell carcinomas and keratoacanthomas. PLX4720 was not itself a true tumor promoter because it could not substitute for the carcinogenesis promoter TPA. Instead, PLX4720 accelerated the growth of preexisting *RAS*-mutant lesions. Taken together with the clinical observations and functional analyses, our data provide circumstantial evidence to suggest that vemurafenib does not initiate tumorigenesis but rather accelerates the progression of preexisting subclinical cancerous lesions with strong upstream MAPK-signaling potential. These findings explain why the lesions generally develop early after vemurafenib treatment and only in a subset of patients. Moreover, we show how RAS-transformed keratinocytes are more proliferative when treated with a BRAF inhibitor *in vitro*.

The timing of the appearance of these lesions after vemurafenib treatment is different from that of secondary neoplasia following cytotoxic chemotherapy. In the case of vemurafenib, the lesions tend to appear within the first few weeks of

treatment, whereas cancers that are due to the genotoxic effects of chemotherapy develop years after exposure. As vemurafenib is highly specific for a small amount of kinases, and RAS mutations arise in SCCs that affect areas where there is previous sun damage, we believe BRAF inhibitors are not directly toxic and carcinogenic but rather are able to potentiate preexisiting preclinical disease that harbour an upstream oncogene.

We also used the skin carcinogenesis model to investigate whether the combination of a BRAF inhibitor with a MAP Kinase downstream inhibitor drug (MEK inhibitor) would be able to abrogate the development of RAS-driven secondary neoplasia in our mice cohorts. The potent and selective MEK inhibitor PD184352 suppressed tumor development by 91% in mice given DMBA, TPA, and PLX4720 but did not mediate tumor remission in mice with established tumors.

These results point to the usefulness of combining a BRAF inhibitor with a MEK inhibitor to prevent the toxic cutaneous side effect, and also suggest we need new BRAF inhibitors that are able to break the paradoxical activation of MAP Kinase pathway in the event of coexisting upstream oncogenic drivers.

Lastly, we found SCC arising in BRAF inhibitor treated animals had a rapid proliferation, as shown in stainings for Ki-67. We observed a 100% rate of response of SCC lesions in mice to the topical application of the antiproliferative FDA approved agent 5-fluorouracil (5FU). Importantly, we show how 2 patients who developed multiple squamoproliferative lesions clinically consistent with KA and early SCC whilst on treatment with the BRAF inhibitor drug dabrafenib responded to topical 5FU presenting complete regression of the keratinocytic lesions. We concluded 5FU is a safe and valid therapeutic alternative to surgery in patients with multiple squamoproliferative lesions arising in the context of BRAF inhibitor therapy. 5FU should be used in cases where lesions are early or too multiple to resect, or where surgery is contraindicated.

Conclusions:

We conclude mouse models are a valuable tool to study melanoma biology.

Understanding the underlying mechanisms of disease and dissecting the relevant pathways implicated in disease onset and progression may ultimately lead to better disease stratification. Mouse models are a successful tool that can be implemented at the preclinical level to predict biology of response to targeted treatments and to understand underlying mechanisms of side effects to targeted drugs.

Our future efforts will aim to use mouse models to understand how recently approved and emerging immunotherapies such as anti-CTLA4 and anti-PD1/PDL1 will target the different subsets of melanoma defined by their oncogenic driver.

REFERENCES:

1. Erdmann, F., et al., *International trends in the incidence of malignant melanoma 1953-2008-are recent generations at higher or lower risk?* Int J Cancer, 2013. **132**(2): p. 385-400.
2. Gray-Schopfer, V., C. Wellbrock, and R. Marais, *Melanoma biology and new targeted therapy.* Nature, 2007. **445**(7130): p. 851-7.
3. Curtin, J.A., et al., *Distinct sets of genetic alterations in melanoma.* N Engl J Med, 2005. **353**(20): p. 2135-47.
4. Curtin, J.A., et al., *Somatic activation of KIT in distinct subtypes of melanoma.* J Clin Oncol, 2006. **24**(26): p. 4340-6.
5. Carvajal, R.D., et al., *KIT as a therapeutic target in metastatic melanoma.* JAMA, 2011. **305**(22): p. 2327-34.
6. Flaherty, K.T. and D.E. Fisher, *New strategies in metastatic melanoma: oncogene-defined taxonomy leads to therapeutic advances.* Clinical cancer research : an official journal of the American Association for Cancer Research, 2011. **17**(15): p. 4922-8.
7. Falchook, G.S., et al., *Dabrafenib in patients with melanoma, untreated brain metastases, and other solid tumours: a phase 1 dose-escalation trial.* Lancet, 2012. **379**(9829): p. 1893-901.
8. Flaherty, K.T., et al., *Inhibition of mutated, activated BRAF in metastatic melanoma.* The New England journal of medicine, 2010. **363**(9): p. 809-19.
9. Flaherty, K.T., et al., *Improved survival with MEK inhibition in BRAF-mutated melanoma.* N Engl J Med, 2012. **367**(2): p. 107-14.

10. Sosman, J.A., et al., *Survival in BRAF V600-mutant advanced melanoma treated with vemurafenib.* N Engl J Med, 2012. **366**(8): p. 707-14.
11. Guo, J., et al., *Phase II, Open-Label, Single-Arm Trial of Imatinib Mesylate in Patients With Metastatic Melanoma Harboring c-Kit Mutation or Amplification.* J Clin Oncol, 2011. **29**: p. 2904-9.
12. Hodi, F.S., et al., *Major response to imatinib mesylate in KIT-mutated melanoma.* J Clin Oncol, 2008. **26**(12): p. 2046-51.
13. Brahmer, J.R., et al., *Safety and activity of anti-PD-L1 antibody in patients with advanced cancer.* N Engl J Med, 2012. **366**(26): p. 2455-65.
14. Topalian, S.L., et al., *Safety, activity, and immune correlates of anti-PD-1 antibody in cancer.* N Engl J Med, 2012. **366**(26): p. 2443-54.
15. Hodi, F.S., et al., *Improved survival with ipilimumab in patients with metastatic melanoma.* N Engl J Med, 2010. **363**(8): p. 711-23.
16. Johannessen, C.M., et al., *COT drives resistance to RAF inhibition through MAP kinase pathway reactivation.* Nature, 2010. **468**(7326): p. 968-72.
17. Chapman, P.B., et al., *Improved survival with vemurafenib in melanoma with BRAF V600E mutation.* N Engl J Med, 2011. **364**(26): p. 2507-16.
18. Heidorn, S.J., et al., *Kinase-dead BRAF and oncogenic RAS cooperate to drive tumor progression through CRAF.* Cell, 2010. **140**(2): p. 209-21.
19. Poulikakos, P.I., et al., *RAF inhibitor resistance is mediated by dimerization of aberrantly spliced BRAF(V600E).* Nature, 2011. **480**(7377): p. 387-90.
20. Landi, M.T., et al., *MC1R germline variants confer risk for BRAF-mutant melanoma.* Science, 2006. **313**(5786): p. 521-2.
21. Viros, A., et al., *Improving melanoma classification by integrating genetic and morphologic features.* PLoS Med, 2008. **5**(6): p. e120.
22. Dhomen, N., et al., *Oncogenic Braf induces melanocyte senescence and melanoma in mice.* Cancer Cell, 2009. **15**(4): p. 294-303.

IMPACT FACTORS

Journal of Investigative Dermatology (2011) impact factor 6.314

New England Journal of Medicine (2011) impact factor 53.298

^{V600E}*Braf::Tyr-CreERT2::K14-Kitl* Mice Do Not Develop Superficial Spreading-Like Melanoma: Keratinocyte Kit Ligand Is Insufficient to "Translocate" ^{V600E}Braf-Driven Melanoma to the Epidermis

Journal of Investigative Dermatology (2012) **132,** 488–491; doi:10.1038/jid.2011.341; published online 24 November 2011

TO THE EDITOR

Transgenic mouse models of melanoma driven by melanocyte-specific expression of oncogenes have been developed to study gene–gene and gene–environment interactions (Damsky and Bosenberg, 2010). Oncogene expression can be constitutive or inducible, but is generally insufficient for melanomagenesis unless tumor-suppressor genes are deleted (*Pten*, *Tp53*, *Cdkn2a*), or the mice are exposed to mutagens such as UV light. Critically, in mice melanoma is largely restricted to the dermal layers of the skin and the epidermis is rarely involved, whereas human cutaneous malignant melanoma generally develops in the epidermis and then invades the deeper layers of skin. This difference presumably occurs because mouse melanocytes are predominantly located in the follicles and dermis and provide pelt pigmentation, whereas human melanocytes are predominantly epidermal and provide protection from UV light.

Melanocyte location in the skin is controlled by the KIT ligand (KITL). Human keratinocytes express KITL throughout life and melanocytes persist in the epidermis. In postnatal mouse skin, KITL expression is restricted to the hair matrix (Yoshida *et al.*, 2001) and the melanocytes are largely located in the follicles. However, if mouse keratinocytes are engineered to express KITL using the *keratin-14* gene promoter (*K14-Kitl*), a proportion of the melanocytes remain in the epidermis throughout life (Kunisada *et al.*, 1998). Using this approach, melanoma driven by tyrosinase-expressed ^{Q61K}Nras (*Tyr-*^{Q61K}*Nras*), p19^{Arf} deletion, and neonatal UV light exposure can be translocated to the mouse epidermis (Walker *et al.*, 2011).

The protein kinase BRAF is mutated in about half of human melanomas and we developed a ^{V600E}Braf-driven mouse melanoma model using the tamoxifen-activated Cre-recombinase/*loxP* technology (Dhomen *et al.*, 2009). ^{V600E}Braf-driven melanomas are exclusively dermal (Dhomen *et al.*, 2009); therefore we tested whether a membrane-bound version of KITL under the control of the *K14* promoter could translocate these tumors to the epidermis. All animal procedures were approved by the local animal ethics committee (ICR) in accordance with the Home Office regulations under the Animals (Scientific Procedures) Act of 1986 (Workman *et al.*, 2010). When *LSL-*^{V600E}*Braf::Tyr-CreERT2* (henceforth ^{V600E}*Braf*) mice were crossed with *K14-Kitl* mice, we observed S100-positive melanocytes in the basal layers of the interfollicular epidermis (Figure 1a) and melanin capping of the nuclei in the keratinocytes (Figure 1b). These features were absent in ^{V600E}*Braf* mice (Figures 1a and b). As previously described (Dhomen *et al.*, 2009), ^{V600E}Braf induced mild hyperpigmentation of the ears and feet (Figure 1c). Notably, KITL also induced increased pigmentation of the feet and ears and ^{V600E}Braf further enhanced this effect (Figure 1c).

^{V600E}Braf also induced nevi comprising pigmented epithelioid and dendritic melanocytes in the deep reticular dermis and hypodermis of the skin (Figure 1d; see Dhomen *et al.*, 2009). However, in ^{V600E}*Braf::K14-Kitl* mice, ^{V600E}Braf induced highly cellular nevi presenting large populations of pigment-laden epithelioid and dendritic melanocytes that occasionally formed ill-defined nests (Figure 1d; Supplementary Figure S1 online). Nevi in ^{V600E}*Braf::K14-Kitl* mice were located in the papillary and reticular dermis and were separated from the epidermis by a narrow Grenz zone. They occasionally reached the hypodermis surrounding the adnexae, but did not present an epidermal component (Figure 1d; Supplementary Figure S1 online).

^{V600E}Braf also induced rapidly growing skin tumors in ^{V600E}*Braf* and ^{V600E}*Braf::K14-Kitl* mice (Figure 2a). The tumors from the two strains of mice were macroscopically similar, but developed with a significantly lower latency in the ^{V600E}*Braf::K14-Kitl* mice (4.8 compared with 12.5 months; log-rank test $P<0.0001$; Figure 2b). ^{V600E}*Braf::K14-Kitl* mice also showed greater tumor penetrance (100% in 7 months compared with 70% in 24 months; Figure 2b) and developed a greater number of tumors (average 3 compared with 0.78; Figure 2c).

Using PCR, we showed that *LSL-*^{V600E}*Braf* was recombined in tumors from ^{V600E}*Braf::K14-Kitl* mice (Figure 2d), and using RT-PCR we confirmed the expression of the melanocytic markers tyrosinase, silver (gp100), Mitf-M, Dct (Trp2), Sox10, Pax3, and Pou3f2 (Brn2; Figure 2e). S100 expression was confirmed by immunostaining (Figure 2f). These data are consistent with a diagnosis of malignant melanoma. The smaller, less advanced tumors presented an intact epidermis and pigmented melanocytes in the reticular dermis, suggestive of residual intradermal nevi (Figure 2g). These lesions were generally amelanotic, paucicellular, and composed of spindle/dendritic

Abbreviations: EtOH, ethanol; KITL, KIT ligand; mGluR1, metabotropic glutamate receptor-1

melanocytes occupying the deeper layers of skin (Figure 2h). The larger lesions were generally asymmetric, poorly circumscribed, and within the superficial dermis (Figure 2i). Prominent ulceration and effacement of the epidermis were common (Figure 2j), as was locally destructive invasion into the subcutaneous layers (Figure 2i and k). These tumors were also generally amelanotic, with rare pigmented melanocytes occupying the superficial aspects. The deeper aspects were composed of atypical spindle melanocytes occasionally arranged in storiform patterns (Figure 2l). Mitotic figures were abundant (Figure 2m). Crucially, as in ^{V600E}*Braf* mice (Dhomen *et al.*, 2009), the tumors in ^{V600E}*Braf::K14-Kitl* mice were exclusively dermal; neither epidermal invasion nor a junctional component was observed (Figures 2g, i, j, and l), and we note that *K14-Kitl* also failed to translocate melanoma driven by the metabotropic glutamate receptor-1 (mGluR1) to the epidermis (Abdel-Daim *et al.*, 2010).

We set out to translocate ^{V600E}*Braf* tumors to the epidermis using *K14-Kitl*. We cannot discount the possibility that rare melanoma cells did colonize the epidermis, but overall the ^{V600E}*Braf::K14-Kitl* melanomas appeared to be exclusively dermal. This may be because, although melanocytes do occupy the epidermis of ^{V600E}*Braf::K14-Kitl*

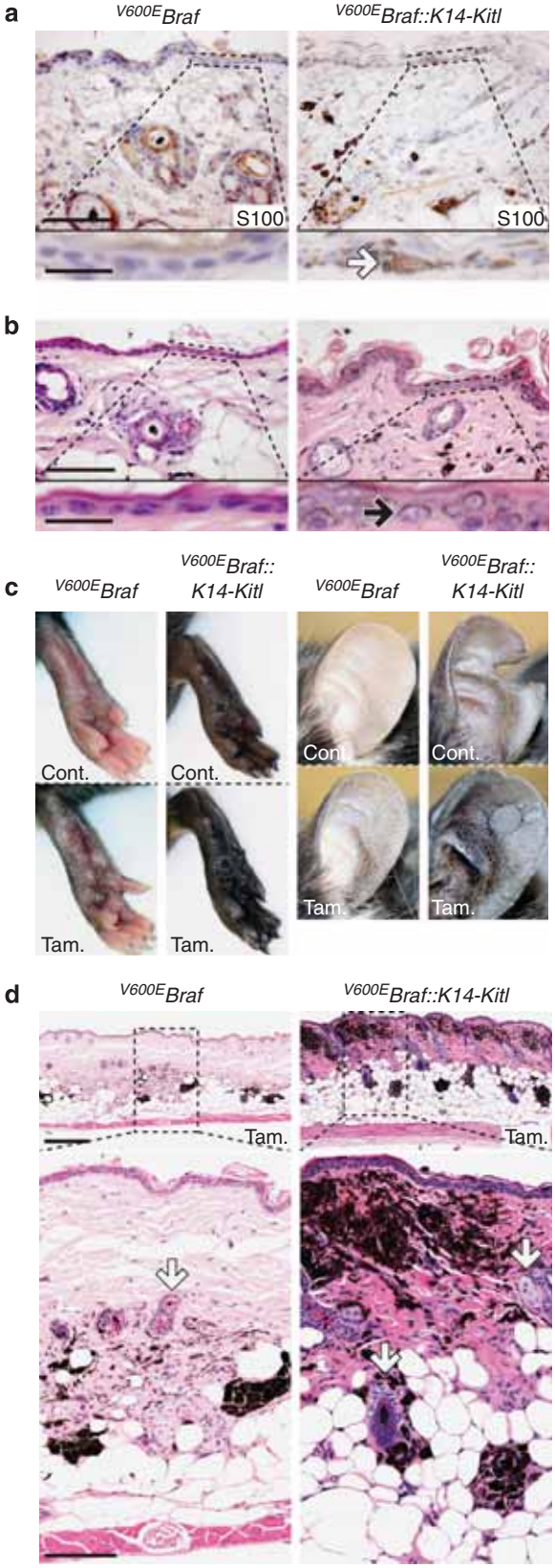

Figure 1. Skin phenotype comparisons in ^{V600E}*Braf* and ^{V600E}*Braf::K14-Kitl* mice before and after tamoxifen treatment. (**a**) Photomicrographs showing S100 staining in skin sections from control (EtOH-treated) ^{V600E}*Braf* and ^{V600E}*Braf::K14-Kitl* mice. The boxed region in the upper panels is enlarged below the images. White arrow shows the presence of S100-positive cells in the epidermis. Upper panel: bar = 150 μm, lower panel: bar = 50 μm. (**b**) Hematoxylin and eosin (H&E) staining of skin sections from control ^{V600E}*Braf* and ^{V600E}*Braf::K14-Kitl* mice. The boxed region in the upper panels is enlarged below the images. Black arrow indicates keratinocyte with melanin cap. Upper panel: bar = 150 μm, lower panel: bar = 50 μm. (**c**) Photographs showing footpads and ears of ^{V600E}*Braf* and ^{V600E}*Braf::K14-Kitl* mice approximately 4 months after EtOH control (Cont.) or tamoxifen (Tam.) treatment. Dashed lines indicate adjacent panel regions that were cropped from the same photograph and processed as a single image. (**d**) H&E staining of skin sections and dermal nevi from tamoxifen-treated ^{V600E}*Braf* and ^{V600E}*Braf::K14-Kitl* mice. The boxed region in the upper panels is enlarged below the images. White arrows indicate skin adnexae (hair follicles and associated sebaceous glands). Upper panel: bar = 0.5 cm, lower panel: bar = 200 μm.

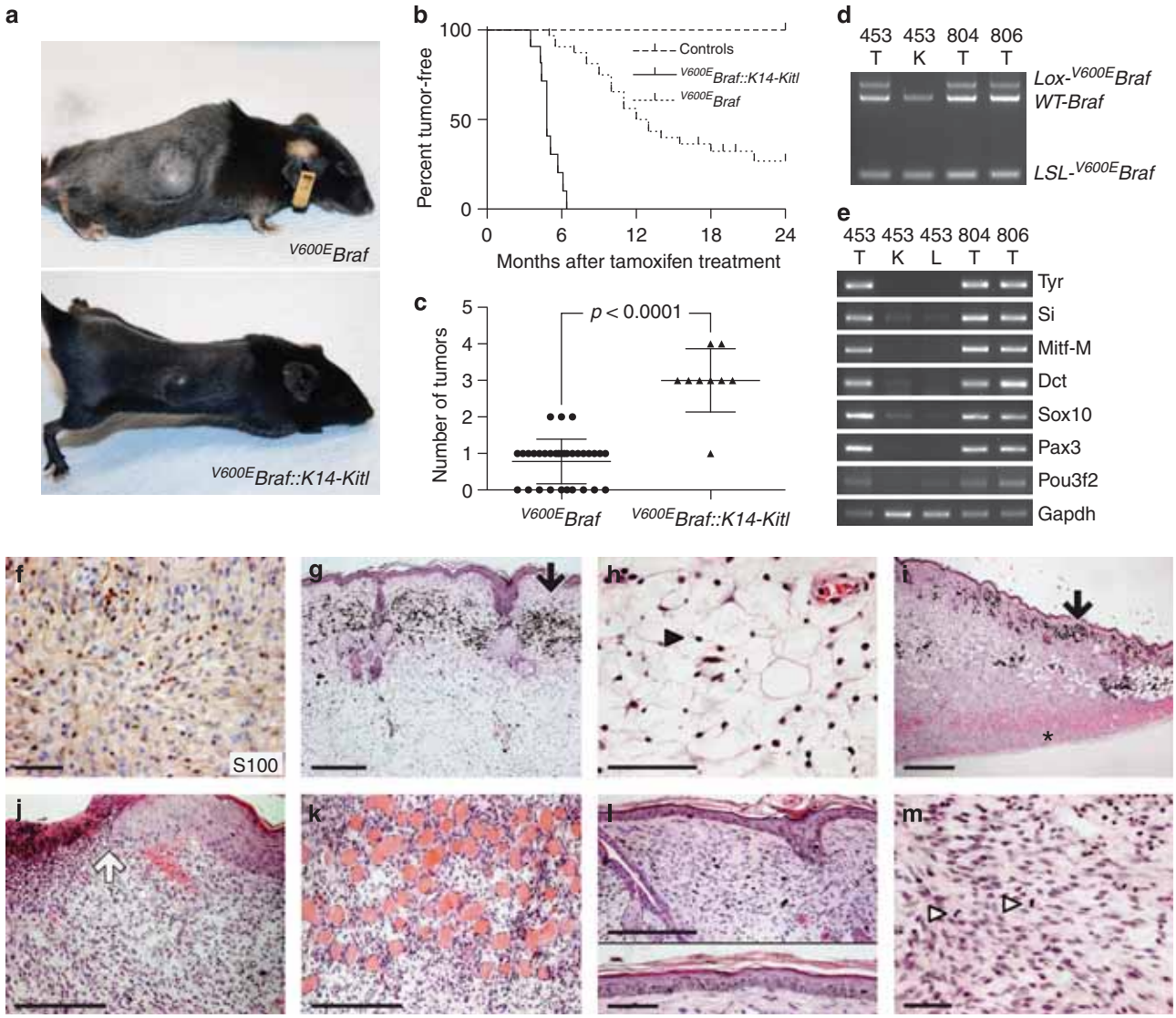

Figure 2. Melanocyte-specific *V600EBraf* expression leads to development of skin tumors in *V600EBraf* and *V600EBraf::K14-Kitl* mice characteristic of malignant melanoma. (**a**) Photographs of *V600EBraf* and *V600EBraf::K14-Kitl* mice presenting skin tumors at similar stages of development. (**b**) Kaplan–Meier curve showing tumor-free survival in *V600EBraf* ($n=32$), *V600EBraf::K14-Kitl* mice ($n=12$), and controls ($n=16$, comprising EtOH-treated *V600EBraf::K14-Kitl* and tamoxifen-treated *K14-Kitl::Tyr-CreERT* mice). The difference between the *V600EBraf* and *V600EBraf::K14-Kitl* curves is statistically significant ($P<0.0001$; Mantel–Cox log-rank test). (**c**) Scatter plot showing tumor number at point of cull, due to tumor burden or having reached the end of the 24-month experimental period, in *V600EBraf* ($n=32$) and *V600EBraf::K14-Kitl* mice ($n=12$). The *P*-value was calculated using Student's *t*-test. (**d**) PCR-mediated genotyping of tumors (T) or kidney (K) from three *V600EBraf::K14-Kitl* mice (no. 453, no. 804, and no. 806). The positions of the wild-type *Braf* allele (*WT-Braf*), the unrecombined *LSL-V600EBraf* allele (*LSL-V600EBraf*), and the recombined *LSL-V600EBraf* allele (*Lox-V600EBraf*) are indicated. (**e**) RT-PCR analysis for tyrosinase (Tyr), silver (Si), melanocyte-specific MITF (Mitf-M), Dct, Sox10, Pax3, Pou3f2, and Gapdh (loading control) in tumors (T), kidney (K), or liver (L) from three *V600EBraf::K14-Kitl* mice (no. 453, no. 804, and no. 806). (**f**) Photomicrograph showing S100-positive nuclear and cytoplasmic staining of *V600EBraf::K14-Kitl* tumor. Bar = 50 μm. (**g**) Photomicrograph of the hematoxylin and eosin (H&E)-stained section showing intact epidermis, dermal localization of the tumor, and dermal nevus remnants (black arrow). Bar = 200 μm. (**h**) Photomicrograph of H&E-stained section showing paucicellular spindle and dendritic cell (black arrowhead) composition of early tumor in the dermis. Bar = 50 μm. (**i**) Low-magnification photomicrograph of the H&E-stained section of an asymmetric, locally aggressive *V600EBraf::K14-Kitl* tumor. Black arrow indicates the presence of the intact epidermis and a nevus remnant in the reticular dermis. Asterisk indicates the presence of deep local invasion of the muscular layer. Bar = 0.5 mm. (**j**) Photomicrograph of the H&E-stained section showing tumor ulceration (white arrow), the absence of epidermal involvement in adjacent epidermis, and increased cellularity in an advanced tumor. Bar = 300 μm. (**k**) Photomicrograph of the H&E-stained section showing deep local invasion of the muscular layer. Bar = 300 μm. (**l**) Photomicrographs showing localization of tumors in the dermis and the absence of epidermal involvement. Upper panel: bar = 300 μm, lower panel: bar = 50 μm. (**m**) Photomicrograph of the H&E-stained section showing increased cellularity in the more advanced lesions. Cells adopt a spindle-shaped morphology and a high number of mitoses are evident (white arrowheads). Bar = 50 μm.

mice, ~90% of the melanocytes remain dermal (Supplementary Figure S2 online); therefore, the probability of developing dermal melanoma may simply be higher. However, we examined 30 tumors and ~50 nevi and found no evidence of epidermal lesions, suggesting that these are not chance events and that even when expressing KITL, the

mouse epidermis does not provide the microenvironment necessary for ^{V600E}B-raf-driven melanomagenesis.

There are several plausible explanations as to why epidermal melanoma developed in the *Tyr-*^{Q61K}*Nras::p19*$^{Arf-/-}$*::K14-Kitl*, but not in the ^{V600E}*Braf::K14-Kitl* or *mGluR1::K14-Kitl* mice. UV light is critical for efficient melanomagenesis in *Tyr-*^{Q61K}*Nras::p19*$^{Arf-/-}$ mice (Ferguson *et al.*, 2010) and has been shown to recruit melanocytes to the epidermis of neonatal mice (Walker *et al.*, 2009). Perhaps the exogenous KITL traps these newly recruited melanocytes and simply increases the chance that epidermal melanoma will develop, or perhaps it provides a microenvironment that supports melanomagenesis in this population in this location. Alternatively, differences in the timing of oncogene expression (prenatal in *Tyr-*^{Q61K}*Nras::p19*$^{Arf-/-}$ mice, induced in juveniles in ^{V600E}*Braf::K14-Kitl* and *mGluR1::K14-Kitl* mice), whether *p19*^{Arf} is deleted or not, or the genetic background of the mice (pure C57BL6 compared with mixed FVB/C57BL6) could account for the differences. Clearly, these are testable hypotheses and, although the KITL did not translocate ^{V600E}Braf melanoma to the epidermis, it increased tumor penetrance and reduced tumor latency and does therefore provide a considerably more robust and versatile mouse model of melanoma.

CONFLICT OF INTEREST

The authors state no conflict of interest.

ACKNOWLEDGMENTS

This work was supported by Cancer Research UK (refs: C107/A10433) and the Institute of Cancer Research. JSR-F is in part funded by the Breakthrough Breast Cancer Research Centre and is a recipient of the 2010 CRUK Future Leaders Prize. We acknowledge NHS funding to the NIHR Biomedical Research Centre. We thank Dr B Jack Longley (University of Wisconsin, Madison) for providing the K14-Kitl mice and also thank Mr Eric Ward (ICR), Dr Kay Savage, and Ms Annette Lane (ICR) for their technical assistance with histological preparations.

***Joel Rae*[1]*, Amaya Viros*[1,2]*, Robert Hayward*[1]*, Dorothy C. Bennett*[3]*, Nathalie Dhomen*[1]*, B Jack Longley*[4]*, Jorge S. Reis-Filho*[5] *and Richard Marais*[1]**

[1]Division of Cancer Biology, The Institute of Cancer Research, London, UK; [2]Departament de Medicina, Seccio Dermatologia, Hospital Vall d'Hebron, Universitat Autonoma de Barcelona, Barcelona, Spain; [3]Molecular Cell Biology Group, Box JBA, Biomedical Sciences Research Centre, St George's University of London, London, UK; [4]Department of Dermatology, University of Wisconsin, Madison, Wisconsin, USA and [5]Molecular Pathology Team, Breakthrough Breast Cancer Research Centre, The Institute of Cancer Research, London, UK
E-mail: Richard.Marais@icr.ac.uk

SUPPLEMENTARY MATERIAL

Supplementary material is linked to the online version of the paper at http://www.nature.com/jid

REFERENCES

Abdel-Daim M, Funasaka Y, Komoto M *et al.* (2010) Pharmacogenomics of metabotropic glutamate receptor subtype 1 and *in vivo* malignant melanoma formation. *J Dermatol* 37:635–46

Damsky WE Jr, Bosenberg M (2010) Mouse melanoma models and cell lines. *Pigment Cell Melanoma Res* 23:853–9

Dhomen N, Reis-Filho JS, da Rocha Dias S *et al.* (2009) Oncogenic Braf induces melanocyte senescence and melanoma in mice. *Cancer Cell* 15:294–303

Ferguson B, Konrad Muller H, Handoko HY *et al.* (2010) Differential roles of the pRb and Arf/p53 pathways in murine naevus and melanoma genesis. *Pigment Cell Melanoma Res* 23:771–80

Kunisada T, Lu SZ, Yoshida H *et al.* (1998) Murine cutaneous mastocytosis and epidermal melanocytosis induced by keratinocyte expression of transgenic stem cell factor. *J Exp Med* 187:1565–73

Walker GJ, Kimlin MG, Hacker E *et al.* (2009) Murine neonatal melanocytes exhibit a heightened proliferative response to ultraviolet radiation and migrate to the epidermal basal layer. *J Invest Dermatol* 129:184–93

Walker GJ, Soyer HP, Handoko HY *et al.* (2011) Superficial spreading-like melanoma in Arf(−/−)::Tyr-Nras(Q61K)::K14-Kitl mice: keratinocyte kit ligand expression sufficient to ''translocate'' melanomas from dermis to epidermis. *J Invest Dermatol* 131:1384–7

Workman P, Aboagye EO, Balkwill F, *et al.*, Committee of the National Cancer Research Institute (2010) Guidelines for the welfare and use of animals in cancer research. *Br J Cancer* 102:1555–77

Yoshida H, Kunisada T, Grimm T *et al.* (2001) Review: melanocyte migration and survival controlled by SCF/c-kit expression. *J Investig Dermatol Symp Proc* 6:1–5

Absence of Mismatch Repair Deficiency–Related Microsatellite Instability in Non-Melanoma Skin Cancer

Journal of Investigative Dermatology (2012) **132,** 491–493; doi:10.1038/jid.2011.326; published online 20 October 2011

TO THE EDITOR

Two major phenotypes of genetic instability characterize cancer cells. Although the majority of cancers are hallmarked by large chromosomal alterations and aneuploidy, some cancers are diploid or near diploid, but show insertion/deletion mutations at repetitive sequences, termed as microsatellites (de la Chapelle, 2003).

The pathogenetic mechanism associated with microsatellite instability at multiple microsatellite loci in cancer (high-level microsatellite instability, MSI-H) is deficient of the DNA mismatch repair (MMR) system (de la Chapelle, 2003). Functional MMR assures correct replication of DNA sequences and is essentially relevant for the correction of mismatches resulting from polymerase slippage at

Abbreviations: BCC, basal cell carcinoma; MMR, mismatch repair; MSI-H, high-level microsatellite instability; NMSC, non-melanoma skin cancer; SCC, squamous cell carcinoma

SUPPLEMENTARY FIGURE LEGENDS

Supplementary Figure 1. *^{V600E}Braf::K14-Kitl* mice develop intradermal nevi.

Photomicrographs showing high power magnification of benign cellular nevi from *^{V600E}Braf::K14-Kitl* mice. The images show the presence of a benign proliferation of mixed epithelioid (white arrowhead) and spindle (black arrowhead) melanocytes within the reticular dermis, but no junctional dermo-epidermal component. Melanophages are evident (black arrow), and the presence of melanocyte nests (asterisk). Scale bar: 50 μm.

Supplementary Fig 2. Melanocytes localize to the basal layer of the epidermis in *^{V600E}Braf::K14-Kitl* mice.

a. Photomicrograph showing S100 staining of normal skin from a *^{V600E}Braf* mouse. White arrowheads indicate follicular melanocytes. Scale bar: 50 μm.

b. Photomicrograph showing S100 staining of normal skin from a *^{V600E}Braf::K14-Kitl* mouse. White arrowheads indicate follicular melanocytes and black arrowheads demonstrate the presence of interfollicular, epidermal melanocytes. Scale bar: 50 μm.

Supplementary Figure 1

^{V600E}Braf::K14-Kitl

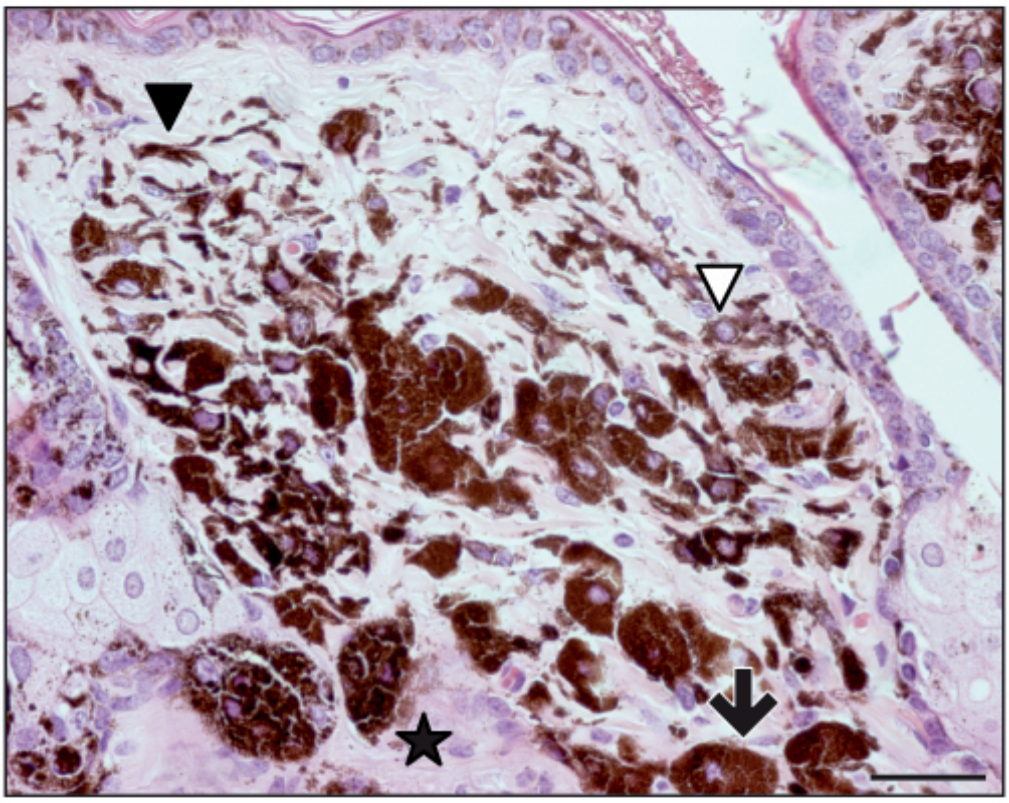

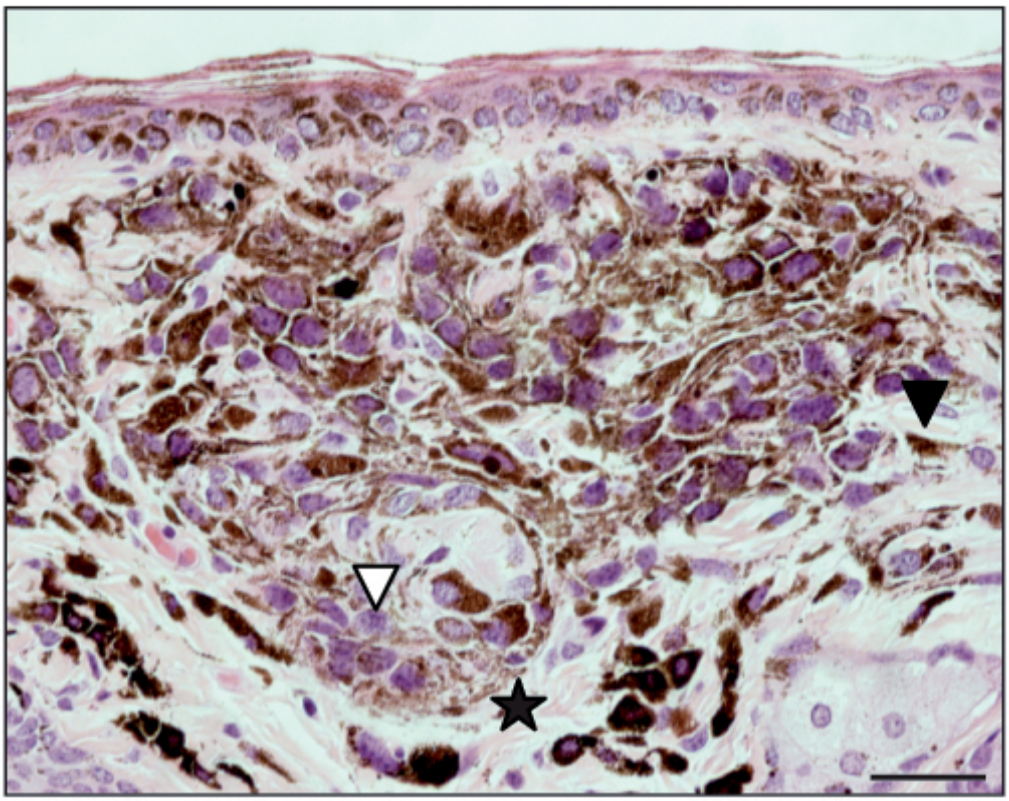

Supplementary Figure 2

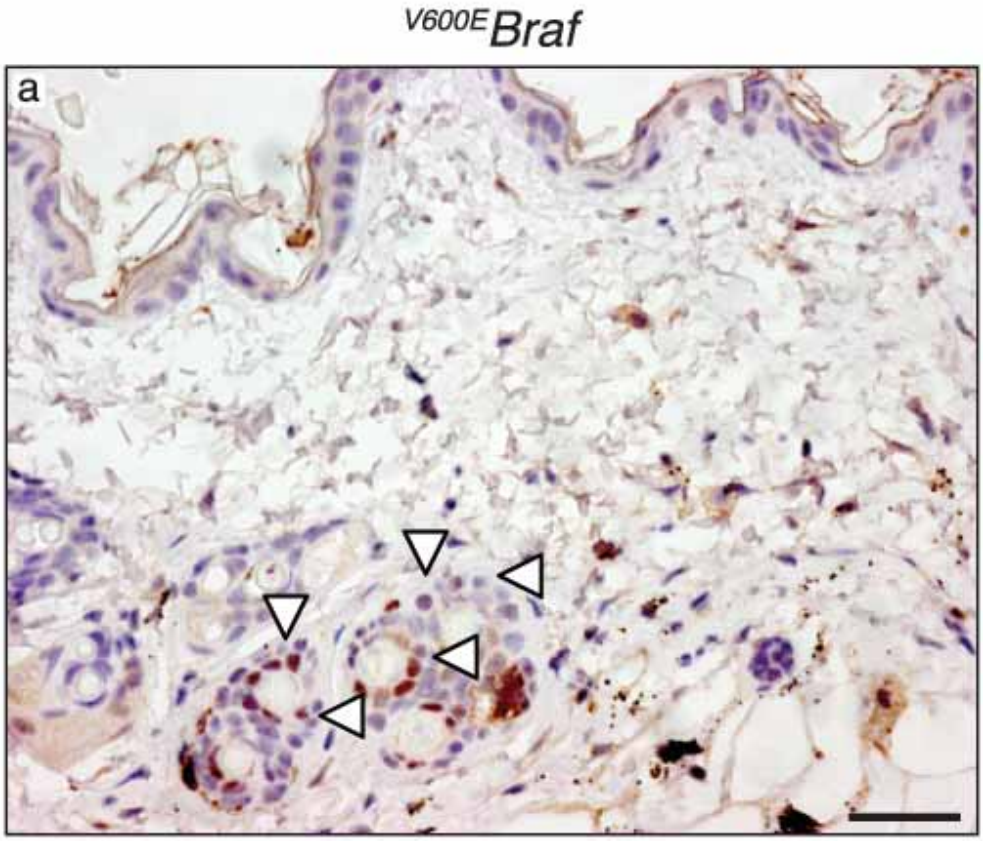

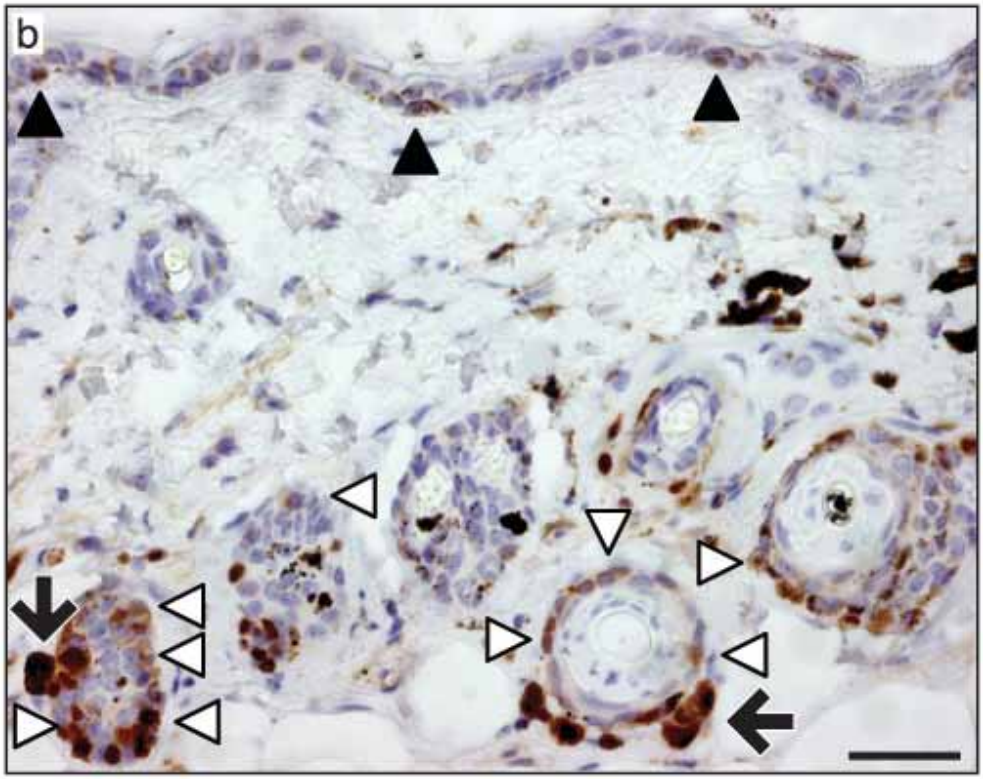

EXPERIMENTAL PROCEDURES

All animal procedures were performed in accordance with National Home Office regulations under the Animals (Scientific Procedures) Act 1986, with ethical approval from the Institute of Cancer Research's Animal Ethics Committee and using the guidance of the Committee of the National Cancer Research Institute (Workman *et al.*, 1988). Genotyping of $^{LSL\text{-}V600E}$*Braf::Tyr-ERT2* mice was as described (Dhomen *et al.*, 2009). Genotyping of the *K14-Kitl* transgene expression was performed by PCR with the primers 5'- GGATTATCACTTGCATTTATCTTC and 5'- GGATCTAGTTTCTGGCCTCTTCGGAG. Tamoxifen (T5648, Sigma-Aldrich) was prepared and applied as described (Dhomen *et al.*, 2009). Histology and S100 immunostaining approaches were as described, as were RT-PCR approaches (Dhomen *et al.*, 2009). For RT-PCR the following primers were used:

Tyr F 5'-GAGTTTGACCCAGTATGAATC and R 5'-CCTGTACTTGGGACATTGTTC,

Si F 5'-TTTATGTTTGGAAGACCTGGG and R 5'-TCCGTCCAAGGCCTGTAGCTG,

Mitf-M F 5'-ATGCTGGAAATGCTAGAATACAGT and R 5'-ATCATCCATCTGCATGCAC,

Dct F 5'-TTTCTAGAGGGCAGGGGGCAG and R 5'-GGTCCAGCCGAACTTGCAGCC,

Sox10 F 5'-TAGCCGACCAGTACCCTCACC and R 5'-CGCCGAGGTTGGTACTTGTAG,

Pax3 F 5'-GAGAACCCGGGCATGTTTAGC and R 5'-CCTTTCTAGATCCGCCTCCTC,

Pou3f2 F 5'-ACGGTGAACGGCATGCTGGGC and R 5'-GTCGTGGTGCGCGCCTGGGTG,

Gapdh F 5'-GGTGAAGGTCGGTGTTGAACGG and R 5'-TTGAATTTGCCGTGAGTGGAG.

The NEW ENGLAND JOURNAL of MEDICINE

ESTABLISHED IN 1812 JANUARY 19, 2012 VOL. 366 NO. 3

RAS Mutations in Cutaneous Squamous-Cell Carcinomas in Patients Treated with BRAF Inhibitors

Fei Su, Ph.D., Amaya Viros, M.D., Carla Milagre, Ph.D., Kerstin Trunzer, Ph.D., Gideon Bollag, Ph.D., Olivia Spleiss, Ph.D., Jorge S. Reis-Filho, M.D., Ph.D., Xiangju Kong, M.S., Richard C. Koya, M.D., Ph.D., Keith T. Flaherty, M.D., Paul B. Chapman, M.D., Min Jung Kim, Ph.D., Robert Hayward, B.S., Matthew Martin, Ph.D., Hong Yang, M.S., Qiongqing Wang, Ph.D., Holly Hilton, Ph.D., Julie S. Hang, M.S., Johannes Noe, Ph.D., Maryou Lambros, Ph.D., Felipe Geyer, M.D., Nathalie Dhomen, Ph.D., Ion Niculescu-Duvaz, Ph.D., Alfonso Zambon, Ph.D., Dan Niculescu-Duvaz, Ph.D., Natasha Preece, B.A., Lídia Robert, M.D., Nicholas J. Otte, B.A., Stephen Mok, B.A., Damien Kee, M.B., B.S., Yan Ma, Ph.D., Chao Zhang, Ph.D., Gaston Habets, Ph.D., Elizabeth A. Burton, Ph.D., Bernice Wong, B.S., Hoa Nguyen, B.A., Mark Kockx, M.D., Ph.D., Luc Andries, Ph.D., Brian Lestini, M.D., Keith B. Nolop, M.D., Richard J. Lee, M.D., Andrew K. Joe, M.D., James L. Troy, M.D., Rene Gonzalez, M.D., Thomas E. Hutson, M.D., Igor Puzanov, M.D., Bartosz Chmielowski, M.D., Ph.D., Caroline J. Springer, Ph.D., Grant A. McArthur, M.B., B.S., Ph.D., Jeffrey A. Sosman, M.D., Roger S. Lo, M.D., Ph.D., Antoni Ribas, M.D., Ph.D., and Richard Marais, Ph.D.

ABSTRACT

BACKGROUND

Cutaneous squamous-cell carcinomas and keratoacanthomas are common findings in patients treated with BRAF inhibitors.

METHODS

We performed a molecular analysis to identify oncogenic mutations (*HRAS*, *KRAS*, *NRAS*, *CDKN2A*, and *TP53*) in the lesions from patients treated with the BRAF inhibitor vemurafenib. An analysis of an independent validation set and functional studies with BRAF inhibitors in the presence of the prevalent *RAS* mutation was also performed.

RESULTS

Among 21 tumor samples, 13 had *RAS* mutations (12 in *HRAS*). In a validation set of 14 samples, 8 had *RAS* mutations (4 in *HRAS*). Thus, 60% (21 of 35) of the specimens harbored *RAS* mutations, the most prevalent being *HRAS Q61L*. Increased proliferation of *HRAS Q61L*–mutant cell lines exposed to vemurafenib was associated with mitogen-activated protein kinase (MAPK)–pathway signaling and activation of ERK-mediated transcription. In a mouse model of *HRAS Q61L*–mediated skin carcinogenesis, the vemurafenib analogue PLX4720 was not an initiator or a promoter of carcinogenesis but accelerated growth of the lesions harboring *HRAS* mutations, and this growth was blocked by concomitant treatment with a MEK inhibitor.

CONCLUSIONS

Mutations in *RAS*, particularly *HRAS*, are frequent in cutaneous squamous-cell carcinomas and keratoacanthomas that develop in patients treated with vemurafenib. The molecular mechanism is consistent with the paradoxical activation of MAPK signaling and leads to accelerated growth of these lesions. (Funded by Hoffmann–La Roche and others; ClinicalTrials.gov numbers, NCT00405587, NCT00949702, NCT01001299, and NCT01006980.)

From Hoffmann–La Roche, Nutley, NJ (F.S., M.J.K., H.Y., Q.W., H.H., J.S.H., B.L., R.J.L., A.K.J.); the Institute of Cancer Research, London (A.V., C.M., J.S.R.-F., R.H., M.M., M.L., F.G., N.D., I.N.-D., A.Z., D.N.-D., N.P., C.J.S., R.M.); Hospital Vall d'Hebron, Universitat Autònoma de Barcelona, Barcelona (A.V.); Hoffmann–La Roche, Basel, Switzerland (K.T., O.S., J.N.); Plexxikon, Berkeley, CA (G.B., Y.M., C.Z., G.H., E.A.B., B.W., H.N., K.B.N.); University of California Los Angeles and the Jonsson Comprehensive Cancer Center, Los Angeles (X.K., R.C.K., L.R., N.J.O., S.M., B.C., R.S.L., A.R.); Massachusetts General Hospital and Harvard Medical School, Boston (K.T.F.); Memorial Sloan-Kettering Cancer Center, New York (P.B.C.); Peter MacCallum Cancer Centre, East Melbourne, VIC, Australia (D.K., G.A.M.); HistoGeneX, Antwerp, Belgium (M.K., L.A.); Medical College of Wisconsin, Milwaukee (J.L.T.); University of Colorado Cancer Center, Aurora (R.G.); Texas Oncology–Baylor Charles A. Sammons Cancer Center, Dallas (T.E.H.); and Vanderbilt University, Nashville (I.P., J.A.S.). Address reprint requests to Dr. Ribas at the Department of Medicine, Division of Hematology–Oncology, 11-934 Factor Bldg., UCLA Medical Center, 10833 Le Conte Ave., Los Angeles, CA 90095-1782, or at aribas@mednet.ucla.edu; or to Dr. Marais at the Institute of Cancer Research. 237 Fulham Rd., London SW3 6JB, United Kingdom, or at richard.marais@icr.ac.uk.

Drs. Su, Viros, and Milagre and Drs. Ribas and Marais contributed equally to this article.

N Engl J Med 2012;366:207-15.

The T→A transversion at position 1799 of *BRAF* (*BRAF V600E*) is present in approximately 50% of patients with metastatic melanoma.[1,2] *BRAF V600E* induces constitutive signaling through the mitogen-activated protein kinase (MAPK) pathway, stimulating cancer-cell proliferation and survival.[2] The clinical development of inhibitors of oncogenic BRAF, termed type I BRAF inhibitors, which block the active conformation of the BRAF kinase, has led to a high rate of objective tumor responses and improvement in overall survival, as compared with standard chemotherapy.[3-5] However, nonmelanoma skin cancers — well-differentiated cutaneous squamous-cell carcinomas and keratoacanthomas — have developed in approximately 15 to 30% of patients treated with type I BRAF inhibitors such as vemurafenib and dabrafenib (GSK-2118436).[3,4,6]

The antitumor activity of vemurafenib against BRAF V600E–mutant cells in cell cultures, animal models, and humans is associated with the inhibition of oncogenic MAPK signaling, as evidenced by the inhibition of phosphorylated ERK (pERK), a downstream effector of BRAF that is active when phosphorylated.[3,7-11] However, BRAF inhibitors induce the opposite effect — that is, increasing pERK in cell lines with wild-type BRAF that harbor upstream pathway activation such as oncogenic RAS or up-regulated receptor tyrosine kinases.[12-14] This RAF inhibitor–dependent activation of MAPK signaling in BRAF wild-type cells is termed paradoxical MAPK-pathway activation[15] and is driven by the formation of RAF dimers that lead to signaling through CRAF and consequently MAPK-pathway hyperactivation.[12-14]

Studies modeling cutaneous squamous-cell carcinomas and keratoacanthomas in mice suggest that these tumors develop from a multistep process whereby an initial carcinogenic event (carcinogenesis inducer), driven by a chemical carcinogen or ultraviolet-light exposure, is followed by a tumor-promoting event.[16] The initiating event in the commonly used two-stage skin carcinogenesis model is an oncogenic driver mutation in *RAS*, preferentially in *HRAS*.[17,18] In humans, sporadic, well-differentiated cutaneous squamous-cell carcinomas and keratoacanthomas harbor *HRAS* mutations at a frequency of 3 to 30%,[19,20] which is less frequent than in the mouse model. In some of these lesions in humans, receptor tyrosine kinases such as the epidermal growth factor receptor (EGFR)[19] are hyperactive, which would also activate RAS and consequently MAPK signaling. Other reported oncogenic events in these lesions in humans include frequent mutations or deletions in *TP53*[21,22] and the cell-cycle control gene *CDKN2A*.

METHODS

PATIENTS AND LESION SAMPLES

Patients participated in the vemurafenib phase 1 dose-escalation study (ClinicalTrials.gov number, NCT00405587), the phase 2 study (NCT00949702), the phase 3 study (NCT01006980), or the drug–drug interaction study (NCT01001299). All patients had BRAF V600–mutant metastatic melanoma and received 720 or 960 mg of vemurafenib orally twice a day. Patients provided written informed consent for molecular analyses of the skin-cancer lesions excised during dermatologic examinations while they were in the study.

MOLECULAR ANALYSES OF TUMOR SPECIMENS

DNA extracted from the tumor specimens was sequenced for *HRAS* (exons 1 and 2), *NRAS* (exons 1 and 2), *KRAS* (exons 1 and 2), and *CDKN2A* (exon 2) with the use of polymerase-chain-reaction (PCR) amplification. (For primers, see Tables 1 and 2 in the Supplementary Appendix, available with the full text of this article at NEJM.org.) This was followed by Sanger sequencing[23] (see the Methods section in the Supplementary Appendix). Single-base substitutions or deletions in *TP53* exons 2 through 11 were analyzed with the use of an investigational AmpliChip p53 Test (Roche Molecular Systems), according to the manufacturer's instructions. ERK phosphorylation was assessed by means of immunohistochemical analysis.

CELLULAR ANALYSES OF THE INTERACTION BETWEEN MUTANT HRAS AND BRAF INHIBITORS

The *HRAS*-mutant B9 murine cutaneous squamous-cell carcinoma cell line was seeded in soft agar with vemurafenib, with the analogue tool compound PLX4720 (both from Plexxikon), or with dimethylsulfoxide (Sigma-Aldrich) vehicle control, for studies of anchorage-independent clonal growth, as described previously.[11] A431 human squamous-cell carcinoma cells (ATCC) either were transfected with empty vector or a plasmid carrying *HRAS Q61L* with the use of Fugene 6 (Roche Molecular Systems), according to the manufacturer's instructions, or were stably transduced with a control or *HRAS Q61L* lentiviral vector, as described previ-

ously.[24] Cells were analyzed for proliferation after vemurafenib exposure by means of cell-viability counts or MTT or MTS assays, as described previously.[9,11,25] NIH3T3 cells (ATCC) were transfected with empty vector or an *HRAS Q61L* plasmid with the use of Fugene 6 and analyzed for colony formation in a soft agar.[11] Western blotting was performed as described previously.[9,11,25] At least two independent experiments were performed in triplicate with the use of each model.

ANALYSIS OF GENE EXPRESSION

B9 cells were plated in dimethylsulfoxide control or 1 μM of vemurafenib or PLX4720 and incubated for 16 hours. Cells were harvested, total RNA was isolated (RNeasy Mini Kit, Qiagen), and gene expression was measured with the use of Affymetrix Mouse 420 2.0 array chips, according to the manufacturer's instructions. Vemurafenib and PLX4720 response genes were identified as those that changed by a factor of more than 2 (up-regulated) or less than 0.5 (down-regulated) relative to controls. The gene patterns of the B9 cells were compared with MAPK-pathway output genes from five human melanoma cell lines,[7] and differential gene expression was confirmed by PCR assay.

STUDIES IN MICE

The procedures in animals were performed in accordance with local animal ethics committees. The two-stage skin carcinogenesis procedures were essentially those that have been described previously,[16,26] with six animals per group. The BRAF inhibitor PLX4720 and the MEK inhibitor PD184352 were synthesized at the Institute of Cancer Research and delivered by means of oral gavage (25 mg per kilogram of body weight per day) in 200 μl of dimethylsulfoxide in water (1:19 solution).

STUDY OVERSIGHT

Data generated and collected by the study investigators were analyzed by the senior academic and industry authors, who vouch for the completeness and accuracy of the analyses and reported results. The clinical protocol summaries for the four trials are available at NEJM.org.

STATISTICAL ANALYSIS

Results of mutation testing in the initial 21 specimens of cutaneous squamous-cell carcinoma lesions of the keratoadenoma subtype and in 14 independent validation specimens are presented as mutation frequencies with 95% confidence intervals. Statistical analysis of gene-expression profiling was performed with the use of the z-test and chi-square analysis with Yates' correction. Analysis of the cell-line culture experiments was performed with the use of Student's t-test and a two-way analysis of variance with a Bonferroni post-test analysis. In the studies of mice, analysis of variance was performed with the use of the Kruskal–Wallis test.

RESULTS

CHARACTERISTICS OF THE PATIENTS AND LESIONS

As part of the dermatopathological review of vemurafenib-treated patients, 21 centrally confirmed samples of cutaneous squamous-cell carcinoma or keratoacanthoma obtained from 11 patients with metastatic melanoma were analyzed (Table 3A in the Supplementary Appendix). A validation set of 14 samples from 12 vemurafenib-treated patients was subsequently analyzed to confirm the high frequency of *RAS* mutations (Table 3B in the Supplementary Appendix). Overall, the mean time to diagnosis of the first cutaneous squamous-cell carcinoma or keratoacanthoma in the combined series was 10 weeks, with the earliest lesion appearing at 3 weeks (Table 4 in the Supplementary Appendix). The mean age at diagnosis was 60 years (range, 44 to 84). Eighteen of the 23 patients (78%) had a history and clinical signs of chronically sun-damaged skin, and 4 (17%) had a history of cutaneous squamous-cell carcinomas or keratoacanthomas. The lesions were widely distributed, with 34% on the head and neck areas, 23% on the torso, and 43% on the extremities. Twenty-two lesions (63%) were characterized as keratoacanthomas (Fig. 1, and Fig. 1 in the Supplementary Appendix), and 13 (37%) were cutaneous squamous-cell carcinomas.

GENE MUTATIONS AND ERK ACTIVATION IN LESION SPECIMENS

In the initial cohort of 21 centrally analyzed samples, there were 14 mutations in hotspot codons (12, 13, and 61) of different *RAS* genes (*HRAS*, *NRAS*, or *KRAS*) in 13 specimens (62%; 95% confidence interval [CI], 38 to 82) (Fig. 1C and 1D and Table 3A in the Supplementary Appendix). The most prevalent *HRAS* substitutions occurred at codon 61 (8 of 14), with fewer at codon 12 (4 of 14) and codon 13 (2 of 14). Two of 18 samples

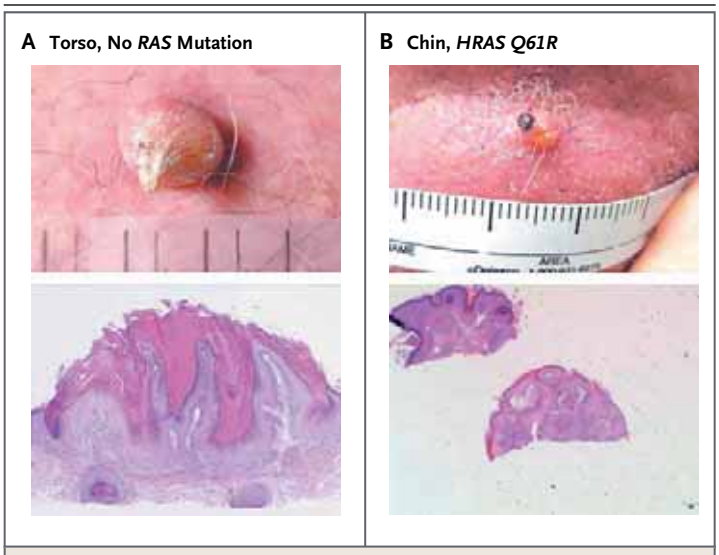

Figure 1. Cutaneous Squamous-Cell Carcinomas or Keratoacanthomas in Patients Treated with Vemurafenib.

Representative photographs and photomicrographs of nonmelanoma skin lesions in vemurafenib-treated patients are shown. The upper image in Panel A shows a lesion with the clinical features of keratoacanthoma, noted on day 98 after the patient had begun taking vemurafenib at a dose of 960 mg twice daily, in the centrally analyzed initial series. The lower image in Panel A is a low-power view of a section of a lesion obtained from the skin of the torso of the same patient with no RAS mutation, reported as squamous-cell carcinoma of the keratoacanthoma subtype (hematoxylin and eosin). Panel B shows the clinical appearance (upper image) and histopathological appearance (lower image, hematoxylin and eosin) of a keratoacanthoma from the chin of a patient with HRAS Q61R in the validation series.

had *TP53* mutations that change amino acids in the p53 protein (Table 3A in the Supplementary Appendix). One sample had an intronic mutation in *TP53*, and for 3 samples (all from Patient 4), no results were obtained. No mutations were identified in exon 2 of *CDKN2A*. ERK phosphorylation was assessed in 10 cutaneous squamous-cell carcinomas or keratoacanthomas and the surrounding normal epithelia and was found to be higher in these lesions than in the normal epidermis (Fig. 2A and 2B in the Supplementary Appendix).

In the validation set, *RAS* mutations were noted in 8 of 14 samples (57%; 95% CI, 29 to 82): 4 in *HRAS* and 4 in *KRAS* (Table 3B in the Supplementary Appendix). In the 4 samples with sufficient surrounding normal skin to perform *RAS* mutational analyses, no mutations were detected (Table 3B and Fig. 2C and 2D in the Supplementary Appendix). Staining for pERK, which was performed in 3 of the 4 samples, was more extensive in the cells of the lesions than in those of the surrounding normal skin (Fig. 2). Thus, *RAS* mutations were noted in 60% of the combined series, and *HRAS Q61L* was the most frequent mutation, so oncogenic HRAS was selected for preclinical mechanistic investigations.

EFFECTS OF BRAF INHIBITORS ON CELLS HARBORING HRAS MUTATIONS

Paradoxical Increase in MAPK Signaling and Proliferation of Cells Harboring Mutated HRAS

To investigate the effects of BRAF inhibitors on *HRAS* mutations in cutaneous squamous-cell carcinomas, we used the murine cell line B9, which harbors the *HRAS Q61L* mutation.[27] Exposure of B9 cells to vemurafenib or its analogue PLX4720 stimulated cell proliferation in soft agar (Fig. 3A). To analyze the underlying mechanism, we compared gene-expression profiles of B9 cells before and after they were exposed to vemurafenib (two independent replicates) or PLX4720. An assessment that included a total of 306 gene probes (representing 250 genes) suggested a shared trend in treatment-induced changes in gene expression that included well-characterized MAPK-pathway genes (*Spry2*, *Dusp6*, *Fos*, *Fos11*, and *Egr1*) ($P<0.001$ by z-test of the three data sets) (Fig. 3A in the Supplementary Appendix). Supervised analysis of these changes in the B9 cells exposed to vemurafenib and PLX4720 revealed a change by a factor of two in nine murine homologues of genes that were differentially expressed when BRAF was inhibited in human melanoma cells expressing the *BRAF V600E* mutation ($P<0.001$ by z-test).[7] Because of the different cell lineages in these two studies, this overlap is significant ($P<0.001$ by chi-square analysis with Yates' correction, two-tailed test). For these nine genes, the change in B9 cells was the opposite of the change in the gene signature observed in the human *BRAF V600E* melanoma cells (Fig. 3B) (see Fig. 3B in the Supplementary Appendix for confirmation with the use of the reverse-transcriptase PCR assay), suggesting that the proliferation stimulated by the BRAF inhibitor results from paradoxically increased MAPK-pathway transcriptional effects in cells with mutant *HRAS*.

To further investigate the functional role of the most prevalent mutation, HRAS Q61L was expressed in the human squamous-cell carcinoma cell line A431, which already harbors an amplified *EGFR* but has wild-type *RAS*. Exposure to vemurafenib induced modest proliferation in A431 cells transfected with a control plasmid vector. In A431

cells expressing HRAS Q61L with the use of plasmid transfection, 1 to 3 μM of vemurafenib stimulated cell proliferation, whereas higher concentrations decreased proliferation (Fig. 4A and 4B in the Supplementary Appendix). Similar data were obtained with the expression of HRAS Q61L in A431 cells with the use of lentiviral transduction (Fig. 4C in the Supplementary Appendix). Western blot analysis showed a dose-dependent increase in pERK that was most notable at 24 hours, with a minimal effect on the parallel phosphatidylinositol 3-kinase (PI3K)–AKT signaling pathway (Fig. 5A in the Supplementary Appendix).

Since amplification of *EGFR* in A431 cells may interfere with the effects of vemurafenib on cells expressing oncogenic HRAS, we studied the interaction between HRAS Q61L and vemurafenib in NIH3T3 cells, an immortalized fibroblast cell line with wild-type *RAS* and without *EGFR* amplification. Cells transfected with the use of a control vector did not form colonies; when cells were transfected with *HRAS Q61L*, the size of the colonies increased in a dose-dependent fashion (Fig. 5B in the Supplementary Appendix), with an increase in pERK, after exposure to vemurafenib (Fig. 3C).

These three in vitro models show that vemurafenib stimulates proliferation in cells with mutated *HRAS Q61L* through paradoxical activation of the MAPK pathway, evidenced by increased ERK phosphorylation and increased expression of ERK-regulated genes.

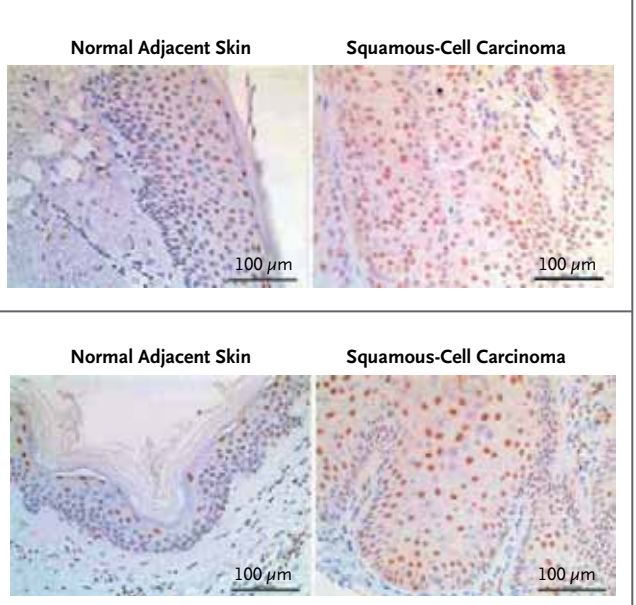

Figure 2. Examples of the Mutation and MAPK-Signaling Analysis in Cutaneous Squamous-Cell Carcinomas or Keratoacanthomas.

Immunohistochemical staining for pERK (brown) of samples of normal adjacent skin (left) and of cutaneous squamous-cell carcinomas (right) is shown from two patients in the validation set who were treated with vemurafenib. In these patients, both of whom had *KRAS G12* mutations, the lesions were diagnosed as well-differentiated squamous-cell carcinomas that appeared 87 days (Panel A) and 51 days (Panel B) after vemurafenib therapy was begun.

PLX4720 and Reduced Tumor Latency in a Mouse Model of Skin Carcinogenesis

To model the in vivo effects of BRAF inhibition in cutaneous squamous-cell carcinomas and keratoacanthomas, we used the two-stage skin carcinogenesis mouse model in which topical application of the carcinogen 7,12-dimethylbenz-(a)anthracene (DMBA) induces *HRAS Q61L* mutations in mouse keratinocytes.[17] Subsequent application of the tumor promoter 12-*O*-tetradecanoyl-phorbol-13-acetate (TPA) then induces these lesions.[17]

In mice that received DMBA and TPA along with PLX4720, the appearance of these lesions was markedly accelerated, as compared with the mice given DMBA and TPA alone (Fig. 4). The addition of PLX4720 did not increase the number of lesions induced by DMBA and TPA, but it reduced tumor latency by 45% and reduced the interval between the initial development of lesions and the maximal tumor burden by 35% ($P=0.002$ by the Kruskal–Wallis test). The lesions arising in the mice given DMBA and TPA alone and in those given DMBA, TPA, and PLX4720 were clinically and histologically similar, consistent with keratoacanthomas and well-differentiated invasive cutaneous squamous-cell carcinomas, and the lesions in both groups of mice had the *HRAS Q61L* mutation (Fig. 6 in the Supplementary Appendix). Mice given the combination of DMBA and PLX4720 alone had no visible or palpable tumors (Fig. 4). For these studies, the analogue compound was used in preference to vemurafenib because it had excellent oral bioavailability in mice, whereas the available formulation of vemurafenib had poor bioavailability when delivered by either the oral or the intravenous route (data not shown).

Suppression of Tumor Development by a MEK Inhibitor

PDV cells are DMBA-transformed mouse keratinocytes that express *HRAS Q61L*.[28] PLX4720 induced pERK and cellular proliferation in PDV cells, and the MEK inhibitor PD184352 blocked pERK acti-

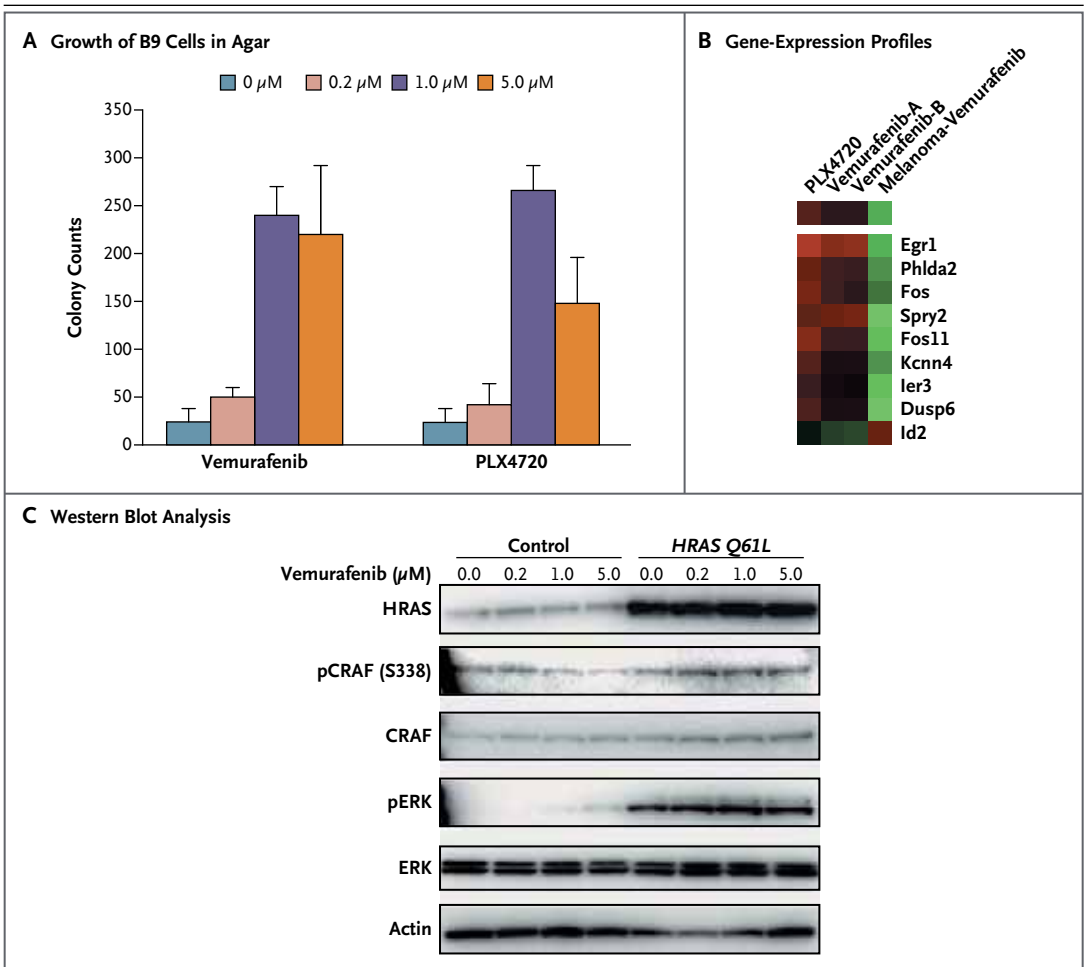

Figure 3. Mechanistic Studies Showing Paradoxical MAPK Activation in Cell Lines.

Panel A shows stimulation of B9 cell growth in soft agar after exposure to vemurafenib or PLX4720. Panel B shows differential expression of selected MAPK-regulated output genes in B9 cells after exposure to vemurafenib or PLX4720 overnight, as compared with gene expression of five human melanoma cell lines used as a reference.[7] Red indicates higher expression and green indicates lower expression than untreated cells. Panel C shows the results of Western blot analysis of NIH3T3 cells transfected with a control vector or with mutated *HRAS Q61L* and treated with different concentrations of vemurafenib.

vation by PLX4720 (Fig. 7A and 7B in the Supplementary Appendix). In the mouse model, PD184352 administration suppressed tumor development by 91% in mice given DMBA, TPA, and PLX4720 (Fig. 4) but did not mediate tumor remission in mice with established tumors (Fig. 7C in the Supplementary Appendix).

DISCUSSION

RAS was the first oncogene discovered in which point mutations led to cellular transformation.[29] Although *RAS* mutations alone typically result in cellular senescence, in conjunction with other events that alter control of the cell cycle and apoptosis, they induce cellular transformation.[30] Mutant *RAS* functions as a driver oncogene in approximately one third of human cancers.[31] The prevalence of *RAS* mutations in sporadic cases of cutaneous squamous-cell carcinomas or keratoacanthomas is not known for sure but reportedly ranges between 3 and 30%.[19,20] Our data indicate that *RAS* mutations are present in approximately 60% of cases in patients treated with vemurafenib, suggesting that preexisting mutations may confer a predisposition to the development of squamous-cell carcinomas or keratoacanthomas. Results of research on the paradoxical activation

of MAPK by RAF inhibitors predicts that upstream oncogenic events, either activating mutations in *RAS* or mutations or amplifications in receptor tyrosine kinases that strongly elevate levels of the RAS–guanosine triphosphate complex in the absence of a *BRAF V600E* mutation, would potentiate signaling through the MAPK pathway.[12-14] Our functional studies showing HRAS-primed activation of the MAPK pathway in models of squamous-cell carcinoma treated with BRAF inhibitors provide evidence that the toxicity related to BRAF inhibition may arise from paradoxical MAPK-pathway activation. Recent studies have shown that vemurafenib resistance can be mediated by receptor tyrosine kinases such as the platelet-derived growth factor and insulin-like growth factor 1 receptors.[32,33] Preexisting amplification of the EGFR gene in the A431 cell-line model also resulted in paradoxical MAPK-pathway signaling in functional assays, although at a lower level than that driven by oncogenic HRAS. These data from in vitro models suggest that similar mutations or amplifications of receptor tyrosine kinases may account for the development of cutaneous squamous-cell carcinomas and keratoacanthomas in the 40% of samples in our combined series in which no *RAS* mutations were found.

The timing of the appearance of these lesions after vemurafenib treatment is decidedly different from that of secondary cancers associated with cytotoxic chemotherapy. In the case of vemurafenib, the lesions tend to appear within the first few weeks after the start of therapy, whereas cancers that are due to the genotoxic effects of chemotherapy develop years after exposure. The specificity of vemurafenib for a limited number of kinases,[8,10] along with our finding that *RAS* mutations occur frequently in lesions arising preferentially in sun-damaged skin, suggests that vemurafenib may not have direct carcinogenic effects but instead may potentiate preexisting initiating oncogenic events.

In the skin carcinogenesis model, the BRAF inhibitor PLX4720 drove paradoxical activation of the MAPK pathway and proliferation of *HRAS Q61L*-transformed keratinocytes, with decreased latency and accelerated growth of cutaneous squamous-cell carcinomas and keratoacanthomas. PLX4720 was not itself a true tumor promoter because it could not substitute for TPA. Instead, PLX4720 accelerated the growth of preexisting *RAS*-mutant lesions. Taken together with the clinical observations and functional analyses, our data provide circumstantial evidence to suggest that vemurafenib does not initiate tumorigenesis but rather accelerates the progression of preexisting subclinical cancerous lesions with strong upstream MAPK-signaling potential. These findings explain why the lesions generally develop early after vemurafenib treatment and only in a subset of patients.

In conclusion, our data provide a molecular mechanism for the development of clinical toxicity that is the opposite of what would be expected from a targeted oncogene inhibitor. This mechanism accounts for the development of cutaneous squamous-cell carcinomas and keratoacanthomas,

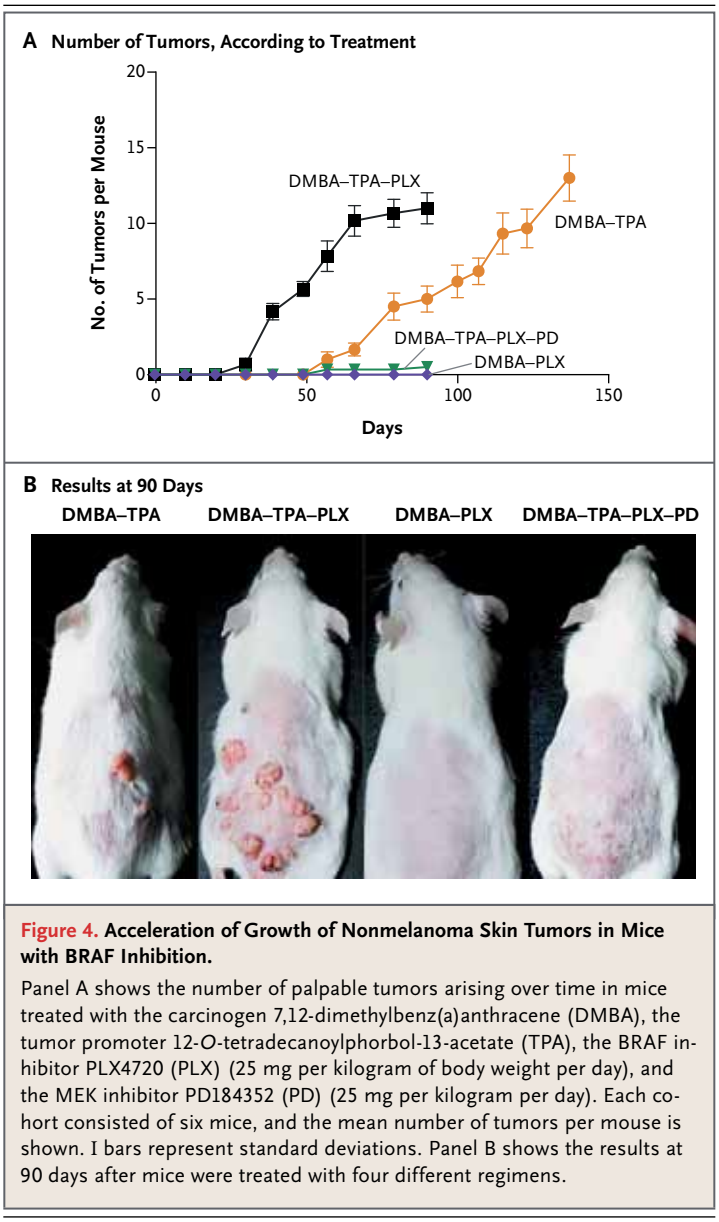

Figure 4. Acceleration of Growth of Nonmelanoma Skin Tumors in Mice with BRAF Inhibition.

Panel A shows the number of palpable tumors arising over time in mice treated with the carcinogen 7,12-dimethylbenz(a)anthracene (DMBA), the tumor promoter 12-*O*-tetradecanoylphorbol-13-acetate (TPA), the BRAF inhibitor PLX4720 (PLX) (25 mg per kilogram of body weight per day), and the MEK inhibitor PD184352 (PD) (25 mg per kilogram per day). Each cohort consisted of six mice, and the mean number of tumors per mouse is shown. I bars represent standard deviations. Panel B shows the results at 90 days after mice were treated with four different regimens.

notably of the skin, but it is not clear whether it is relevant to the development of squamous-cell carcinomas in other organs. Our findings support the caution against investigating single-agent type I BRAF inhibitors in patients with cancers driven by RAS or by activated receptor tyrosine kinases. The discovery that the development of these lesions is driven by RAS and by MAPK in patients receiving BRAF inhibitors, as well as the effects noted in the animal model, point to the usefulness of combining a BRAF inhibitor with a MEK inhibitor to prevent this toxic effect[34] and make way for the clinical development of a new generation of BRAF inhibitors selected to avoid paradoxical MAPK-pathway activation.

Supported in part by Hoffmann–La Roche and Plexxikon (to Drs. Su, Trunzer, and Bollag); the Seaver Institute, the Louise Belley and Richard Schnarr Fund, the Fred L. Hartley Family Foundation, the Wesley Coyle Memorial Fund, the Ruby Family Foundation, the Albert Stroberg and Betsy Patterson Fund, the Jonsson Cancer Center Foundation, and the Caltech–UCLA Joint Center for Translational Medicine (to Drs. Lo and Ribas); the European Organisation for Research and Treatment of Cancer Melanoma Group, Cancer Research U.K. (CRUK) (C107/A10433 and CRUK-A8274), the American Institute for Cancer Research (09-0773), and the Institute of Cancer Research (to Dr. Marais); and Breakthrough Breast Cancer and the 2010 CRUK Future Leaders Prize in Cancer Research (to Dr. Reis-Filho).

Disclosure forms provided by the authors are available with the full text of this article at NEJM.org.

We thank the patients and study investigators for participating in the two studies; the Association for International Cancer Research; Carla Duymelinck, Suzanne Cheng, Jennifer Narozny, Louise Cockey, Astrid Koehler, and Michael Stumm for assisting with organizing and conducting the molecular analyses of patient specimens; Dr. Alain Balmain (University of California, San Francisco) for providing the B9 cells; Dr. Miguel Quintanilla (Madrid) for providing PDV cells; Dr. Kay Savage, Eric Ward, and Annette Lane (Institute of Cancer Research), and Ngan Doan (University of California, Los Angeles), for assisting with histology and immunohistochemistry; and Alice Smith and Vidya Pawar (Institute of Cancer Research) for assisting with DNA sequencing.

REFERENCES

1. Davies H, Bignell GR, Cox C, et al. Mutations of the BRAF gene in human cancer. Nature 2002;417:949-54.
2. Wan PT, Garnett MJ, Roe SM, et al. Mechanism of activation of the RAF-ERK signaling pathway by oncogenic mutations of B-RAF. Cell 2004;116:855-67.
3. Flaherty KT, Puzanov I, Kim KB, et al. Inhibition of mutated, activated BRAF in metastatic melanoma. N Engl J Med 2010; 363:809-19.
4. Ribas A, Kim K, Schuchter L, et al. BRIM-2: an open-label, multicenter Phase II study of RG7204 (PLX4032) in previously treated patients with BRAF V600E mutation-positive metastatic melanoma. J Clin Oncol 2011;29:Suppl:8509. abstract.
5. Chapman PB, Hauschild A, Robert C, et al. Improved survival with vemurafenib in melanoma with BRAF V600E mutation. N Engl J Med 2011;364:2507-16.
6. Kefford R, Arkenau H, Brown MP, et al. Phase I/II study of GSK2118436, a selective inhibitor of oncogenic mutant BRAF kinase, in patients with metastatic melanoma and other solid tumors. J Clin Oncol 2010;28:Suppl:611s. abstract.
7. Joseph EW, Pratilas CA, Poulikakos PI, et al. The RAF inhibitor PLX4032 inhibits ERK signaling and tumor cell proliferation in a V600E BRAF-selective manner. Proc Natl Acad Sci U S A 2010;107: 14903-8.
8. Tsai J, Lee JT, Wang W, et al. Discovery of a selective inhibitor of oncogenic B-Raf kinase with potent antimelanoma activity. Proc Natl Acad Sci U S A 2008; 105:3041-6.
9. Søndergaard JN, Nazarian R, Wang Q, et al. Differential sensitivity of melanoma cell lines with BRAFV600E mutation to the specific raf inhibitor PLX4032. J Transl Med 2010;8:39.
10. Bollag G, Hirth P, Tsai J, et al. Clinical efficacy of a RAF inhibitor needs broad target blockade in BRAF-mutant melanoma. Nature 2010;467:596-9.
11. Yang H, Higgins B, Kolinsky K, et al. RG7204 (PLX4032), a selective BRAFV600E inhibitor, displays potent antitumor activity in preclinical melanoma models. Cancer Res 2010;70:5518-27. [Erratum, Cancer Res 2010;70:9527.]
12. Poulikakos PI, Zhang C, Bollag G, Shokat KM, Rosen N. RAF inhibitors transactivate RAF dimers and ERK signalling in cells with wild-type BRAF. Nature 2010;464:427-30.
13. Hatzivassiliou G, Song K, Yen I, et al. RAF inhibitors prime wild-type RAF to activate the MAPK pathway and enhance growth. Nature 2010;464:431-5.
14. Heidorn SJ, Milagre C, Whittaker S, et al. Kinase-dead BRAF and oncogenic RAS cooperate to drive tumor progression through CRAF. Cell 2010;140:209-21.
15. Hall-Jackson CA, Eyers PA, Cohen P, et al. Paradoxical activation of Raf by a novel Raf inhibitor. Chem Biol 1999;6:559-68.
16. Abel EL, Angel JM, Kiguchi K, DiGiovanni J. Multi-stage chemical carcinogenesis in mouse skin: fundamentals and applications. Nat Protoc 2009;4:1350-62.
17. Quintanilla M, Brown K, Ramsden M, Balmain A. Carcinogen-specific mutation and amplification of Ha-ras during mouse skin carcinogenesis. Nature 1986;322:78-80.
18. Balmain A, Ramsden M, Bowden GT, Smith J. Activation of the mouse cellular Harvey-ras gene in chemically induced benign skin papillomas. Nature 1984;307: 658-60.
19. Uribe P, Gonzalez S. Epidermal growth factor receptor (EGFR) and squamous cell carcinoma of the skin: molecular bases for EGFR-targeted therapy. Pathol Res Pract 2011;207:337-42.
20. Oberholzer PA, Kee D, Dziunycz P, et al. RAS mutations are associated with the development of cutaneous squamous cell tumors in patients treated with RAF inhibitors. J Clin Oncol 2011 November 7 (Epub ahead of print).
21. Alam M, Ratner D. Cutaneous squamous-cell carcinoma. N Engl J Med 2001; 344:975-83.
22. White AC, Tran K, Khuu J, et al. Defining the origins of Ras/p53-mediated squamous cell carcinoma. Proc Natl Acad Sci U S A 2011;108:7425-30.
23. Sanger F, Nicklen S, Coulson AR. DNA sequencing with chain-terminating inhibitors. Proc Natl Acad Sci U S A 1977; 74:5463-7.
24. Koya RC, Kasahara N, Pullarkat V, Levine AM, Stripecke R. Transduction of acute myeloid leukemia cells with third generation self-inactivating lentiviral vectors expressing CD80 and GM-CSF: effects on proliferation, differentiation, and stimulation of allogeneic and autologous antileukemia immune responses. Leukemia 2002;16:1645-54.
25. Niehr F, von Euw E, Attar N, et al. Combination therapy with vemurafenib (PLX4032/RG7204) and metformin in melanoma cell lines with distinct driver mutations. J Transl Med 2011;9:76.
26. González-García A, Pritchard CA, Paterson HF, Mavria G, Stamp G, Marshall CJ. RalGDS is required for tumor forma-

tion in a model of skin carcinogenesis. Cancer Cell 2005;7:219-26.
27. Burns PA, Jack A, Neilson F, Haddow S, Balmain A. Transformation of mouse skin endothelial cells in vivo by direct application of plasmid DNA encoding the human T24 H-ras oncogene. Oncogene 1991;6:1973-8.
28. Quintanilla M, Haddow S, Jonas D, Jaffe D, Bowden GT, Balmain A. Comparison of ras activation during epidermal carcinogenesis in vitro and in vivo. Carcinogenesis 1991;12:1875-81.
29. Sukumar S, Notario V, Martin-Zanca D, Barbacid M. Induction of mammary carcinomas in rats by nitroso-methylurea involves malignant activation of H-ras-1 locus by single point mutations. Nature 1983;306:658-61.
30. Collado M, Gil J, Efeyan A, et al. Tumour biology: senescence in premalignant tumours. Nature 2005;436:642.
31. Malumbres M, Barbacid M. RAS oncogenes: the first 30 years. Nat Rev Cancer 2003;3:459-65. [Erratum, Nat Rev Cancer 2003;3:708.]
32. Nazarian R, Shi H, Wang Q, et al. Melanomas acquire resistance to B-RAF(V600E) inhibition by RTK or N-RAS upregulation. Nature 2010;468:973-7.
33. Villanueva J, Vultur A, Lee JT, et al. Acquired resistance to BRAF inhibitors mediated by a RAF kinase switch in melanoma can be overcome by cotargeting MEK and IGF-1R/PI3K. Cancer Cell 2010; 18:683-95.
34. Infante JR, Falchook GS, Lawrence DP, et al. Phase I/II study to assess safety, pharmacokinetics, and efficacy of the oral MEK 1/2 inhibitor GSK1120212 (GSK212) dosed in combination with the oral BRAF inhibitor GSK2118436 (GSK436). J Clin Oncol 2011;29:Suppl. abstract.

Supplementary Appendix

This appendix has been provided by the authors to give readers additional information about their work.

Supplement to: Su F, Viros A, Milagre C, et al. *RAS* mutations in cutaneous squamous-cell carcinomas in patients treated with BRAF inhibitors. N Engl J Med 2012;366:207-15.

(PDF updated February 2, 2012.)

Table of Contents

Supplemental Information for: Su, Viros, Alegre *et al*. RAS mutations in cutaneous squamous cell carcinomas with BRAF inhibitors

Supplemental Figure Legends

Supplemental Figure 1. Additional examples of cutaneous squamous cell carcinomas or keratoacanthomas (cuSCC/KA) in patients treated with vemurafenib. A and B) Clinical and pathologic presentations and corresponding RAS status (additional details in Supplemental Table 3b; magnification, 1.25X; bar, 100 μM) from two cases in the validation set (A: patient 3, B: patient 10). C and D) Examples of Sanger sequencing of mutations in *HRAS* and *KRAS*: C) Sequencing tracings of a left temple SCC/KA from patient 4 from the initial set demonstrating a $HRAS^{Q61L}$ mutation, but wild type *KRAS*; D) Sequencing tracings of a right cheek SCC/KA from the same patient 4 demonstrating a $KRAS^{G12C}$ mutation, but wild type *HRAS*.

Supplemental Figure 2. Examples of pERK staining and sequencing for *RAS* mutations in cuSCC/KAs and surrounding unaffected skin. A) Lesion from patient 1 of the initial series, a KA from the arm with a $HRAS^{Q61K}$ mutation in a patient without a prior history of cuSCC/KAs. The basal cell layer shows strong pERK staining in cuSCC, with pERK staining present in normal epithelia, but to a lower extent. B) Lesion from patient 7 from the initial series, a cuSCC from the arm in a patient with prior history of other cuSCCs. The lesion demonstrated a $TP53^{P278S}$ mutation and no mutation in *RAS*. This case demonstrates low pERK staining, but it is present in the more differentiated tumor cells. ERK phosphorylation is present in normal epithelia, but to a lower extent, and there is pigmentation in the basal cell layer. C and D) Sequencing traces at the $KRAS^{G12}$ codon demonstrating the presence of a mutation in the cuSCC/KA lesions but not in the normal skin surrounding the lesions.

Supplemental Figure 3. Differential gene expression profiling of murine SCC cells exposed to BRAF inhibitors. A) Comparison of differentially expressed genes in murine B9 cells following overnight exposure to PLX4720 and vemurafenib (in replicates, labeled A and B respectively). Red indicates higher and green indicates lower expression compared to

untreated cells. B) PCR confirmation of differentially expressed genes identified in the gene microarray studies. B9 cells and $BRAF^{V600E}$–expressing melanoma cell lines, A375 and SK-MEL-28 were treated with 0.5 μM of vemurafenib or 1 μM of PLX4720 respectively for 6 or 16 hours, total RNA was extracted then RT-PCR was performed (Applied Biosystems). Each time point and concentration has triplicate samples. Blue bars represent fold changes of genes in the B9 mouse cuSCC cells and red bars represent average fold changes of genes in A375 and SK-MEL-28 human melanoma cell lines.

Supplemental Figure 4. Studies of vemurafenib-induced proliferation and signal transduction in A431 human SCC cells with or without oncogenic $HRAS^{Q61L}$. A and B) A431 cells transfected with $HRAS^{Q61L}$ or a control plasmid were analyzed using the MTT assay (Sigma) for proliferation (A) or by plotting the number of viable cells (B). C) A431 cells stably transduced with a lentiviral vector expressing $HRAS^{Q61L}$ or a control empty lentiviral vector (wt) were treated with increasing doses of vemurafenib for 3 days and analyzed by an MTS-based cell viability assay. Values on the y-axis are the relative proliferation of cells in comparison to vehicle (DMSO) treated cells. Comparisons of replicate samples were statistically significant (all $p < 0.05$) between the vemurafenib concentrations of 0.0005, 0.05 and 2.5 μM (two-way ANOVA with Bonferroni posttest analysis).

Supplemental Figure 5. Additional effects of vemurafenib on signaling and colony growth of $HRAS^{Q61L}$ mutant cells. A) A431 cells stably transduced with a lentiviral vector expressing $HRAS^{Q61L}$ or a control empty lentiviral vector (wt) were treated with vehicle (DMSO) control, 1 or 5 μM vemurafenib for 1 hour or 24 hours. Cells were lysed in cold RIPA buffer with a cocktail of protease/phosphatase inhibitors, and protein concentration was measured by BCA assay (Thermo Scientific, Rockford, IL). 8 μg of total protein was loaded in each well for SDS-PAGE. Total and phosphorylated kinases were assessed by immunoblotting. B) NIH3T3 cells transfected with a control vector or with mutated $HRAS^{Q61L}$ were cultured in increasing concentrations of vemurafenib for soft agar proliferation assay.

Supplemental Figure 6. BRAF inhibition accelerates growth of non-melanoma skin tumors in mice. A) Representative photomicrographs of exophytic papillomas and sharply demarcated exophytic cuSCC/KAs (left and centre panels; scale bars 1mm), with their corresponding dermal invasive fronts (right panels; scale bars 50 um). Arrows indicate deep dermal mitoses. B) Sanger sequencing profiles of representative cuSCC/KAs lesions from mice treated with DMBA/TPA and DMBA/TPA/PLX4720. The position of the CTA codon encoding the *HRAS*^{Q61L} mutation is indicated by the arrow.

Supplemental Figure 7. PLX4720 induces paradoxical activation of the MEK/ERK pathway and stimulates proliferation of *HRAS*^{Q61L}-transformed keratinocytes. A) Western blots for BRAF, CRAF, phosphorylated MEK (pMEK), phosphorylated ERK (pERK) and total ERK2 (loading control) in whole cell lysates from PDV cells treated with DMSO, PD184352 (PD; 2 μM, 60 min) and/or PLX4720 (PLX; 300 nM, 60 min). B) Graph showing proliferation in PDV cells treated with DMSO (control) or PLX4720 (PLX; 300 nM, 96 hours). Error bars represent standard deviation from the mean. C) Graph showing the induction of palpable lesions on the skin of DMBA, TPA and PLX4720-treated mice. Mice in one of the cohorts (represented by the green line) were additionally treated with PD184352 (+PD) after 47 days (indicated by the arrow).

Supplemental Online Methods

cuSCC/KA initial sample collection, processing and analysis

Tissues included in the original and validation sets were recruited independently. Surplus material was obtained following pathological analysis of suspicious lesions excised for clinical purposes. Available samples at the time of analysis were included in both series, with the centrally analyzed series using the first set of samples, and the validation set including samples provided by academic investigators. Samples were sent for centralized dermatopathology and molecular analyses (initial set). Suspicious skin lesions in formalin-fixed paraffin embedded (FFPE) tumor blocks or slides were submitted to a central dermatopatholgy laboratory (Dermpath, Palm Beach Gardens, FL) for histopathological review. Confirmed cuSCC/KA lesions were then forwarded to a central molecular pathology laboratory (HistoGeneX, Berchem, Belgium) for further molecular analyses. A validation set of 14 cases was assembled at three study sites (UCLA, Vanderbilt University and Peter McCallum Cancer Center) from cuSCC/KA biopsies in 12 patients. Samples in the validation set were assessed by the pathology departments of the hospitals of origins and by Dr Jorge Reis-Filho and Dr Amaya Viros to confirm diagnosis. Samples were included if there was a common diagnosis of atypical squamous cell proliferations with a keratoacanthoma-like differentiation or as atypical squamous cell proliferations with a predominantly invasive compartment.

Oncogenic analyses of tumor specimens

DNA was extracted from cuSCC/KA specimens with tumor cell proportion of at least 50% using the QIAamp DNA Mini Kit for FFPE Tissue (Qiagen, Hilden, Germany). *HRAS* (exons 1 & 2), *NRAS* (exons 1 & 2), *KRAS* (exons 1 & 2) and *CDKN2A* (exon 2) gene sequences were analyzed using direct DNA sequencing according to the Sanger technology[22]. For each

normalized sample, 5 ng template DNA was amplified in duplicate in independent polymerase chain reactions (PCR) for the amplicon of interest (Supplemental Table 1). Uracil-DNA glycosylase (UNG) was added to avoid generation of artifacts. The DNA products of the nested PCR reactions were purified and subjected to double strand (forward and reverse) Big Dye Terminator (BDT) cycle sequencing using ABI3730XL DNA Analyzers (Applied Biosystems, Carlsbad, CA). Data were analyzed using Phred, Phrap and Polyphred (University of Washington, Seattle, WA). Optimization studies demonstrated that the sensitivity of the Sanger sequencing procedure is approximately 20% for the detection of somatic mutations in the background of non-mutated DNA (data not shown). Sequence traces were manually reviewed by two qualified persons. Sequence variation was detected in the forward and corresponding reverse reactions and confirmed in either the forward or reverse reaction of the replicate. Single-base substitution or deletion mutations in *TP53* exons 2 through 11 were analyzed in DNA isolated from tumor specimens using the investigational AmpliChip® p53 Test (Roche Molecular Systems, Inc, Pleasanton, CA), which is accomplished through PCR amplification, fragmentation and labeling, then microarray hybridization and scanning.

For the validation set, DNA was extracted following microdissection of tumour samples to ensure neoplastic cell poportion >70%. PCR amplification using the primers described in Supplemental Table 2 was performed to allow direct DNA sequencing. PCR reactions consisted of 40 cycles of 95 degrees C 30'', 55 degrees C 1', 72 degrees C 1', after initial denaturation at 95 degrees C for 5'. PCR products were purified using Quiagen PCR Purification kit and then used as templates for forward and reverse sequencing reactions using Big Dye v3.1 (Applied Biosystems).

Mouse *HRAS* exon 3 was PCR amplified and sequenced from microdissected tumor samples containing >70% neoplastic cells as described[33,34]. PCRs were performed as described above.

For the RT-PCR confirmation of the findings of Affymetric gene microarray data, pre-designed gene expression assays targeting genes were obtained from Applied Biosystems (Foster City, CA). Primers and probes are listed in Supplementary Table 4. All gene expression assays were performed on an ABI PRISM® 7900HT Sequence Detection System (Applied Biosystems, Foster City, CA). Briefly, 1 ug total RNA was used for ss cDNA Synthesis using Quanta qScript cDNA SuperMix (Quanta BioSciences Cat# 95048). PCR mix consisted of 10 µl PerfeCTa® qPCR FastMix, ROX™ (Quanta, Gaithersburg, MD), 1 µl Taqman or custom assay, and 2 µl DEPC-treated water (Ambion, Applied Biosystems, Foster City, CA) for each reaction. cDNA samples were diluted to 10 ng/µl in RNase-free water (Ambion, Applied Biosystems, Foster City, CA), and 7 µl added to a 384-well optical plate (Applied Biosystems, Foster City, CA) containing 13 µl pre-distributed assay PCR mix. Thermocycling conditions consisted of 45 °C for 2 min, 95 °C for 3 min, followed by 40 cycles of 95°C for 15 sec then 60°C for 45 sec using Quanta PerfeCTa qPCR Fast Mix (Quanta BioSciences Cat #95077). Each measurement was performed in triplicate. The expression levels of target genes were normalized to reference gene levels and represented as relative expression (E), $E = 2^{(\Delta Ct)}$, where ΔCt is the difference between reference and target gene cycles at which the amplification exceeds an arbitrary threshold. The level of expression of the target genes were normalized to 4 genes of reference (GOR: 18S, Beta-Actin, GAPDH, and GusB) and the geometric mean* of the 4 GORs.

Additional methods for the tissue culture experiments

The B9 murine cuSCC cell line was cultured in RPMI-1640 medium (Mediatech Inc., Manassas, VA) containing compounds added and changed once a week. After three weeks of exposure, colonies greater than 100 µm in diameter were scored by AxioVision Rel 4.8 software (Carl Zeiss, Wake Forest, NC).

For studies in the mouse cuSCC/KAs cell line PDV, antibodies for CRAF, BRAF, and ERK2 were from Santa Cruz Biotechnology. Phospho-ERK1/2 and tubulin antibodies were from Sigma. PD184352 and PLX4720 were synthesized in-house. PDV cells were maintained in DMEM supplemented with 10% FBS. Cell viability was measured by Cell Titer Glo (Promega) according to the manufacturer's instructions. To prepare cell lysates, cells were washed once with ice-cold PBS and harvested into 500 µl lysis buffer (20 mM Tris-HCl (pH 7.5), 150 mM NaCl, 1 mM EDTA, 1%NP-40, 10 mM NaF, 1 mM Na_3VO_4, 1 mg/ml leupeptin, 1 mg/ml aprotinin) per 10 cm dish. The lysates were cleared of insoluble material by high-speed centrifugation, and protein concentrations were determined by the bicinchoninic acid (BCA) protocol from Pierce (Thermosicentific, UK). For Immunoprecipitations 1 mg of protein lysate was immunoprecipitated for 2 hours with 5 µg CRAF antibody and captured on protein G sepharose beads (Thermosicentific, UK). Western blots were performed by standard techniques and analyzed on an Odyssey Infrared Scanner (Li-COR Biosciences).

Supplemental Table 1. List of Primers used for PCR reactions in the initial series.

Primer name	Gene/Exon	Primer Sequence	Amplicon Length
KRAS2-ex02-F	KRAS exon 2	5'-GTGTGACATGTTCTAATATAGTCA-3'	214
KRAS2-ex02-R		5'-GAATGGTCCTGCACCAGTAA-3'	
KRAS2-ex02N-F	KRAS exon 2	5'-ATGTTCTAATATAGTCACATTTTC-3'	202
KRAS2-ex02N-R		5'-GTCCTGCACCAGTAATATGC-3'	
KRAS2-ex03-F	KRAS exon 3	5'-TAAAAGGTGCACTGTAATAATCC-3'	279
KRAS2-ex03-R		5'-TAAAAACTATAATTACTCCTTAATG-3'	
KRAS2-ex03N-F	KRAS exon 3	5'-CACTGTAATAATCCAGACTGTG-3'	264
KRAS2-ex03N-R		5'-CTATAATTACTCCTTAATGTCAGC-3'	
HRAS-ex02-F	HRAS exon 2	5'-AGGGACCGCTGTGGGTTTGC-3'	379
HRAS-ex02-R		5'-ACAGGGCCACAGCACCATGC-3'	
HRAS-ex02N-F	HRAS exon 2	5'-CTGGCTGAGCAGGGCCCTC-3'	292
HRAS-ex02N-R		5'-CACCATGCAGGGGACCAGG-3'	
HRAS-ex03-F	HRAS exon 3	5'-GAGAGGTACCAGGGAGAGGC-3'	331
HRAS-ex03-R		5'-TGCCTGGACGCAGCCGGCC-3'	
HRAS-ex03N-F	HRAS exon 3	5'-AGGCTGGCTGTGTGAACTCC-3'	312
HRAS-ex03N-R		5'-CTGGACGCAGCCGGCCTGG-3'	
NRAS-ex02-F	NRAS exon 2	5'-CAAATGGAAGGTCACACTAGG-3'	333
NRAS- ex02-R		5'-TTACTTTCTCTCCTCTTATTCC-3'	
NRAS- ex02N-F	NRAS exon 2	5'-ATAGAAAGCTTTAAAGTACTG-3'	275
NRAS- ex02N-R		5'-TTCCTTTAATACAGAATATGG-3'	
NRAS- ex03-F	NRAS exon 3	5'-CCTCCACACCCCCAGGATTC-3'	205
NRAS- ex03-R		5'-GCTCCTAGTACCTGTAGAGG-3'	
NRAS- ex03N-F	NRAS exon 3	5'-CACACCCCCAGGATTCTTAC-3'	190
NRAS- ex03N-R		5'-CTGTAGAGGTTAATATCCGC-3'	
CDKN2A-ex02-I-F	CDKN2A exon 2 -I	5'-AAGCTTCCTTTCCGTCATGC-3'	243
CDKN2A-ex02-I -R		5'-CCCAGGCATCGCGCACGTC-3'	
CDKN2A-ex02-II-F	CDKN2A exon 2 -II	5'-ACTCTCACCCGACCCGTGC-3'	294
CDKN2A-ex02-II -R		5'-GGAAAATGAATGCTCTGAG-3'	
CDKN2A-ex02N-II -F	CDKN2A exon 2 -II	5'-ACCCGACCCGTGCACGACGC-3'	279
CDKN2A-ex02N-II -R		5'-ATGCTCTGAGCTTTGGAAGC-3'	

Supplemental Table 2. List of Primers used for PCR reactions in the validation set.

Primer name	Gene/Exon	Primer Sequence	Amplicon Length
HRAS- codon 12/13-F	HRAS codon 12&13	5'-CAGGAGACCCTGTAGGAGGA-3'	139
HRAS- codon 12/13-R		5'-TCGTCCACAAAATGGTTCTG-3'	
HRAS- codon 61-F	HRAS codon 61	5'-GTGGTCATTGATGGGGAGAC-3'	133
HRAS- codon 61-R		5'TGGTGTTGTTGATGGCAAAC-3'	
KRAS- codon 12/13-F	KRAS codon 12&13	5'TCATTATTTTTATTATAAGGCCTGCTG-3'	185
KRAS- codon 12/13-R		5'AGAATGGTCCTGCACCAGTAA-3'	
KRAS- codon 61-F	KRAS codon 61	5'CCAGACTGTGTTTCTCCCTTC-3'	152
KRAS- codon 61-R		5'AAAGAAAGCCCTCCCCAGT-3'	
NRAS- codon 12/13-F	NRAS códon 12&13	5'GGTTTCCAACAGGTTCTTGC-3'	153
NRAS- codon 12/13-R		5'CACTGGGCCTCACCTCTATG-3'	
NRAS- codon 61-F	NRAS códon 61	5'CACCCCCAGGATTCTTACAG-3'	148
NRAS- codon 61-R		5'TGGCAAATACACAGAGGAAGC-3'	

Supplemental Table 3a. Clinical presentation and oncogenic events in cuSCC/KAs from the initial series of patients treated with vemurafenib

ID	Gender	Age	Chronic sun damaged skin	History of prior SCC/KA	Time from start of therapy until 1st SCC/KA (wks)*	SCC/KA skin location	Pathological characterization	Oncogenic events in cuSCC/KA
1	M	62	Yes	No	16	Arm	SCC-KA subtype	$HRAS^{Q61K}$
2	F	67	Yes	No	11	Head and neck	SCC	None detected
						Torso	SCC-KA subtype	$HRAS^{G12D}$ $NRAS^{G12D}$
3	M	52	No	No	8	Head and neck	SCC-KA subtype	None detected
						Torso	SCC	$HRAS^{Q61R}$
						Leg	SCC-KA subtype	$HRAS^{G12D}$
						Leg	SCC-KA subtype	None detected
						Torso	SCC-KA subtype	$HRAS^{Q61K}$
						Torso	SCC-KA subtype	$HRAS^{Q61L}$
4	M	83	Yes	Yes	6	Head and neck	SCC-KA subtype	$HRAS^{Q61L}$ Intron TP53 mutation
						Arm	SCC-KA subtype	None detected
						Arm	SCC-KA subtype	$HRAS^{G13D}$
						Torso	SCC-KA subtype	$HRAS^{G13V}$

						Head and neck	SCC-KA subtype	$KRAS^{G12C}$ $TP53^{R196X}$
5	M	56	Yes	No	5	Head and neck	SCC	$HRAS^{Q61L}$
6	M	44	Yes	No	8	Leg	SCC-KA subtype	None detected
7	M	60	Yes	Yes	8	Arm	SCC	$TP53^{P278S}$
8	F	53	Yes	No	6	Leg	SCC (with features of KA)	None detected
9	F	54	Yes	No	9	Leg	SCC-KA subtype	$HRAS^{Q61L}$
10	M	71	Yes	No	15	Torso	SCC-KA subtype	None detected
11	M	61	Yes	Yes	15	Arm	SCC-KA subtype	$HRAS^{Q61L}$

*At the time of the first cuSCC/KA all patients were taking vemurafenib 960 mg orally twice daily, except patient #4 who received 720 mg orally twice daily.

Legend: SCC: squamous cell carcinoma; KA: keratoacanthoma.

Supplemental Table 3b. Clinical presentation and oncogenic events in cuSCC/KAs from the validation series of patients treated with vemurafenib

ID	Gender	Age	Chronic sun damaged skin	History of prior SCC/KA	Time from start of therapy until 1st SCC/KA (wks)*	SCC/KA skin location	Pathological characterization	Oncogenic events in cuSCC/KA	RAS mutations in surrounding skin
1	M	80	Yes	No	9	Head and neck	SCC	None detected	ND
2	M	67	No	No	5	Head and neck	SCC	$HRAS^{Q61L}$	Wild type
3	M	69	No	No	9	Torso	SCC-KA subtype	$KRAS^{G12D}$	Wild type
4	F	66	Yes	No	12	Arm	SCC-KA subtype	None detected	ND
5	M	66	Yes	No	12	Torso	SCC-KA subtype	$HRAS^{Q61L}$	ND
6	M	51	No	No	15	Head and neck	SCC-KA subtype	$HRAS^{Q61R}$	ND
7	M	84	Yes	No	18	Arm	SCC	$KRAS^{G12C}$	Wild type
						Leg	SCC	None detected	ND
8	M	62	Yes	No	4	Arm	SCC-KA subtype	None detected	ND
9	F	72	Yes	Yes	6	Leg	SCC	None detected	ND
10	M	46	No	No	22	Head and neck	SCC-KA subtype	$HRAS^{Q61L}$	ND
11	M	55	Yes	No	18	Head and neck	SCC	None detected	ND

						Head and neck	SCC	$KRAS^{G12C}$	Wild type
12	M	84	Yes	No	3	Head and neck	SCC	$KRAS^{G12D}$	ND

Legend: SCC: squamous cell carcinoma; KA: keratoacanthoma; ND: Not done.

Supplemental Table 4. Baseline characteristics of patients with cuSCC/KA lesions.

		Initial series	Validation set	Total
Clinical Trial	Vemurafenib phase 1	7	2	9
	Vemurafenib phase 2	4	7	11
	Vemurafenib phase 3	0	1	1
	Drug-drug interaction study	0	2	2
Gender	Female	3	2	5
	Male	8	10	18
Age	Mean	60	66	60
	Range	44-83	46-84	44-84
Country	Australia	4	1	5
	USA	7	11	18
Number of Reported cuSCC/KA Events	Mean	2	4	3
	Range	1-6	1-10	1-10
Average Time to First Occurrence of cuSCC/KA (weeks)	Mean	9	11	10
	Range	5-16	3-22	3-22
Dose at Day of 1st cuSCC/KA Excision	Vemurafenib 720 mg	1	1	2
	Vemurafenib 920 mg	10	11	21

Supplemental Figure 1

a)

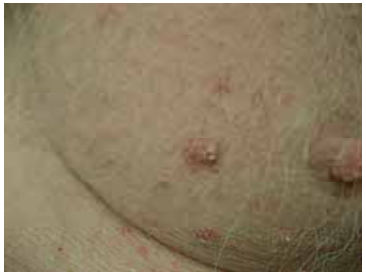

Left chest
KRAS^{G12D}

b)

Left scalp
HRAS^{Q61L}

c)

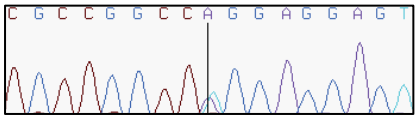

CAG->CTG

HRAS
P.GLN61LEU

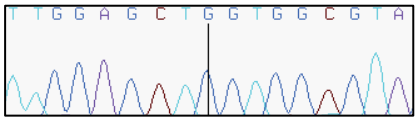

GGT-
>TGT

KRAS
(codon 12)

No mutation

d)

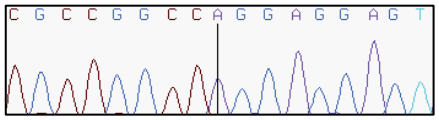

CAG->CTG

HRAS
(codon 61)

No mutation

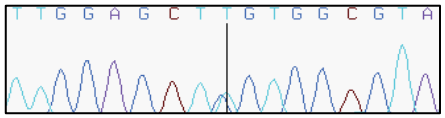

GGT-
>TGT

KRAS
P.GLY12
CYS

Supplemental Figure 2

a)

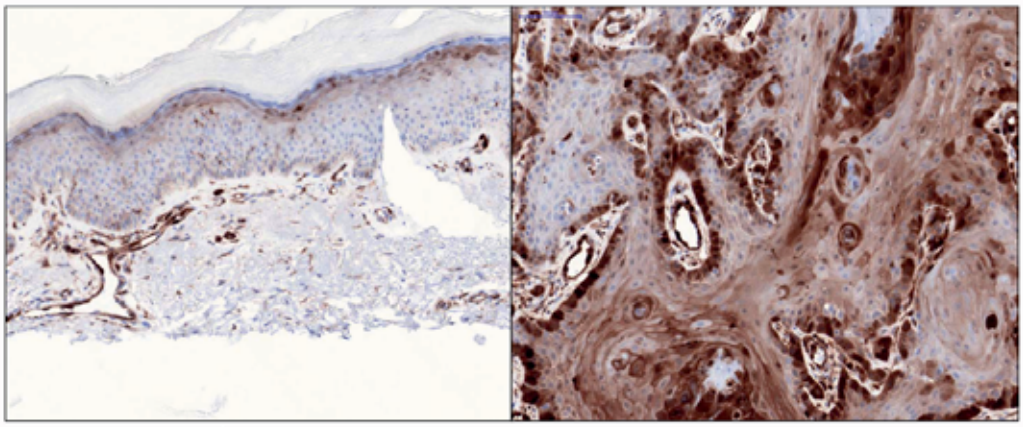

b)

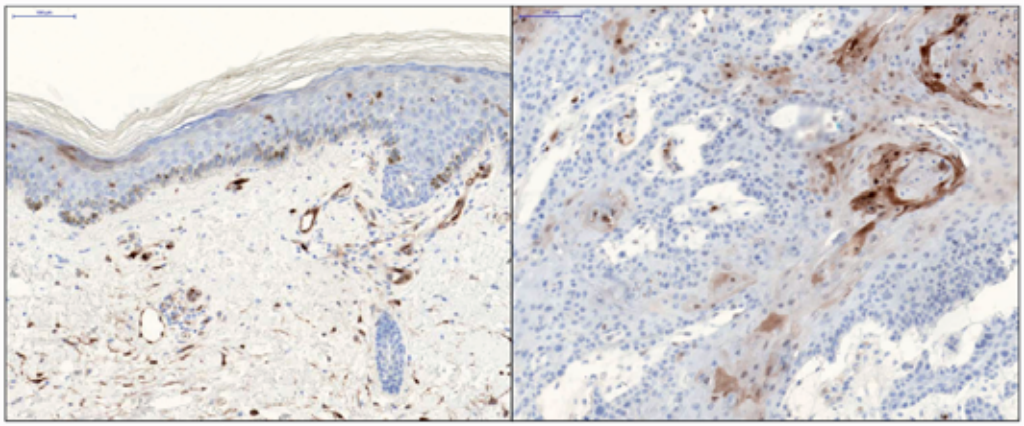

Surrounding skin

cuSCC/KA

c)

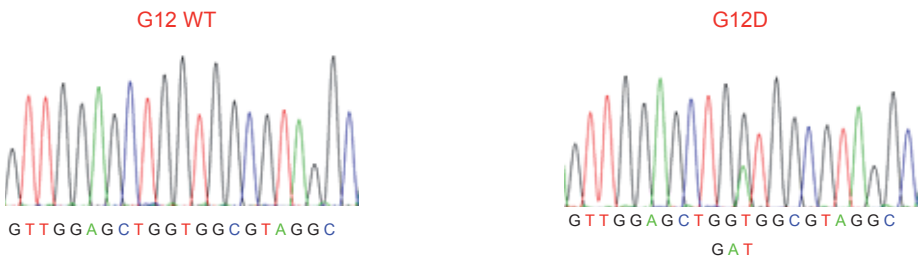

d)

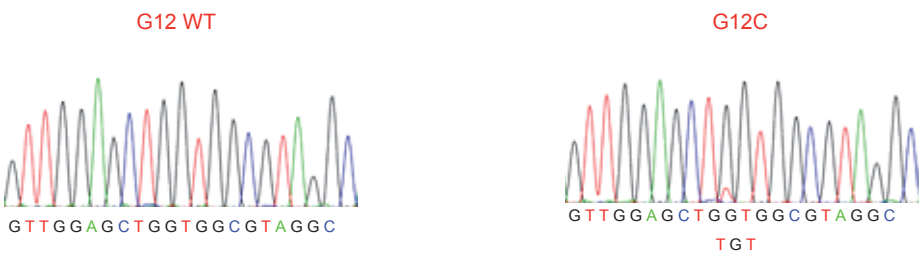

Supplementary Figure 3

a)

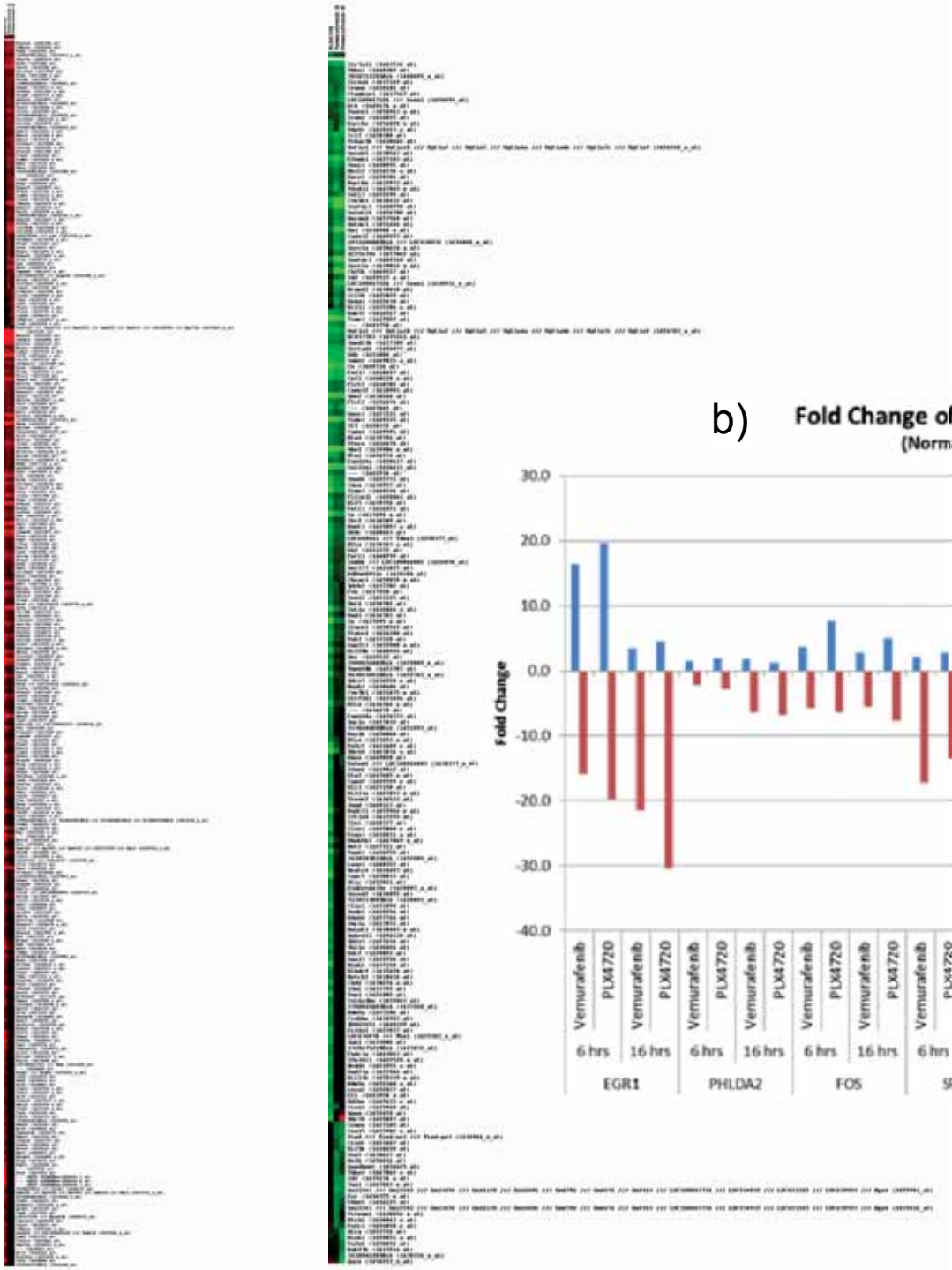

b)

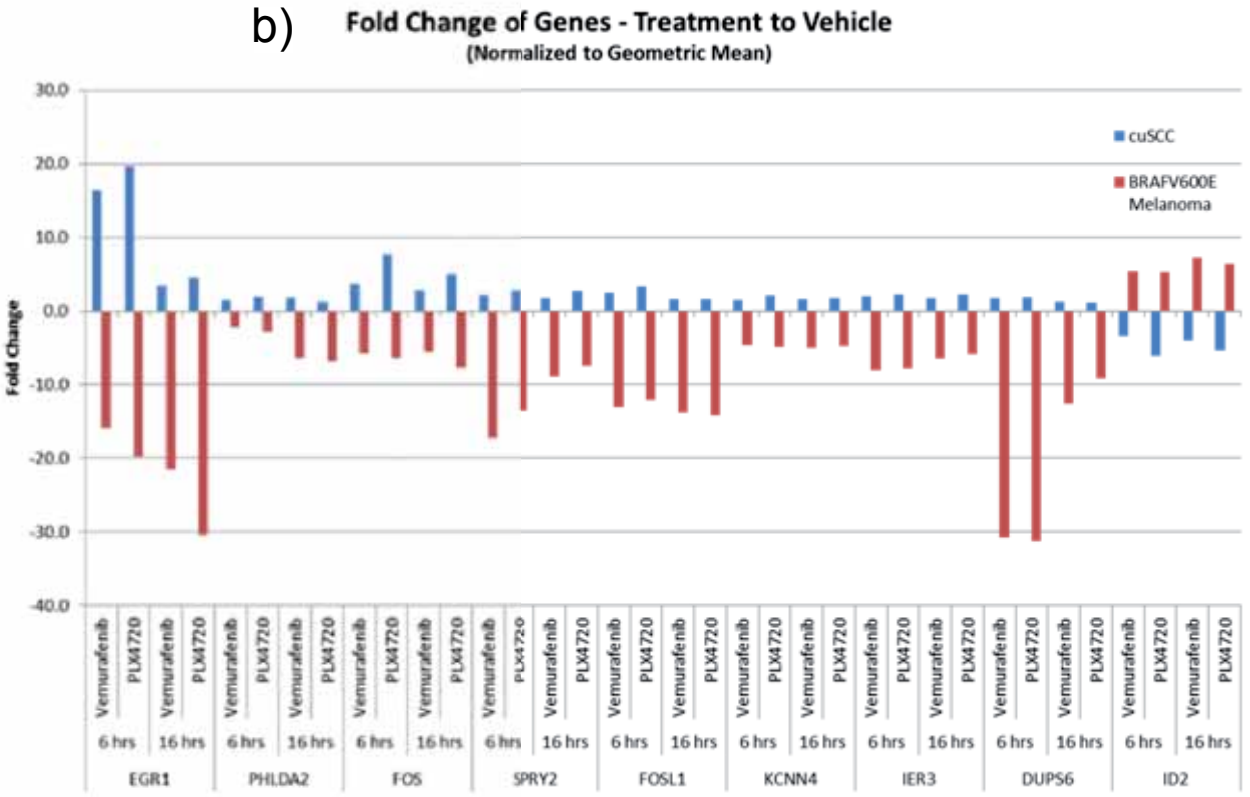

Supplemental Figure 4

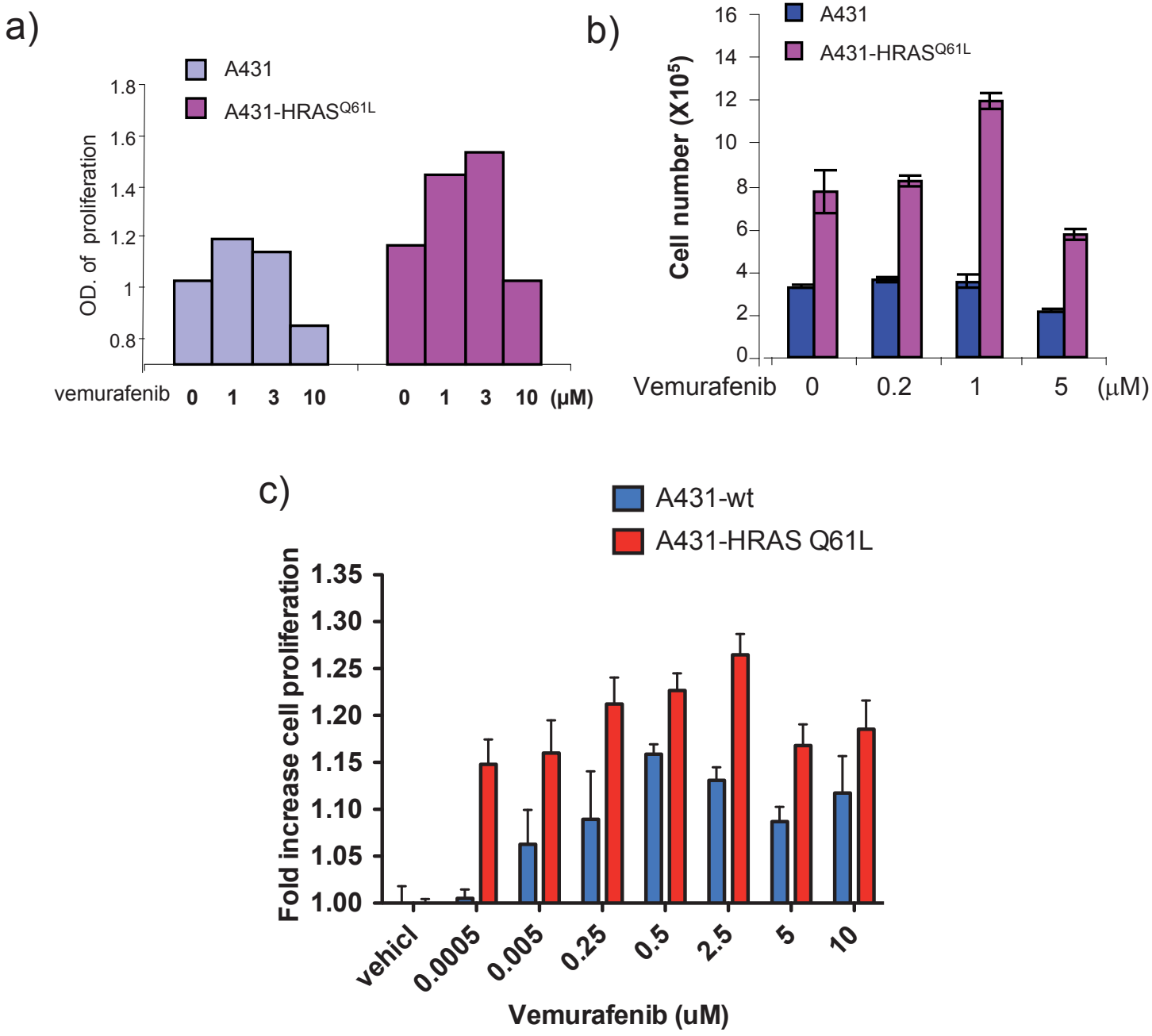

Supplemental Figure 5

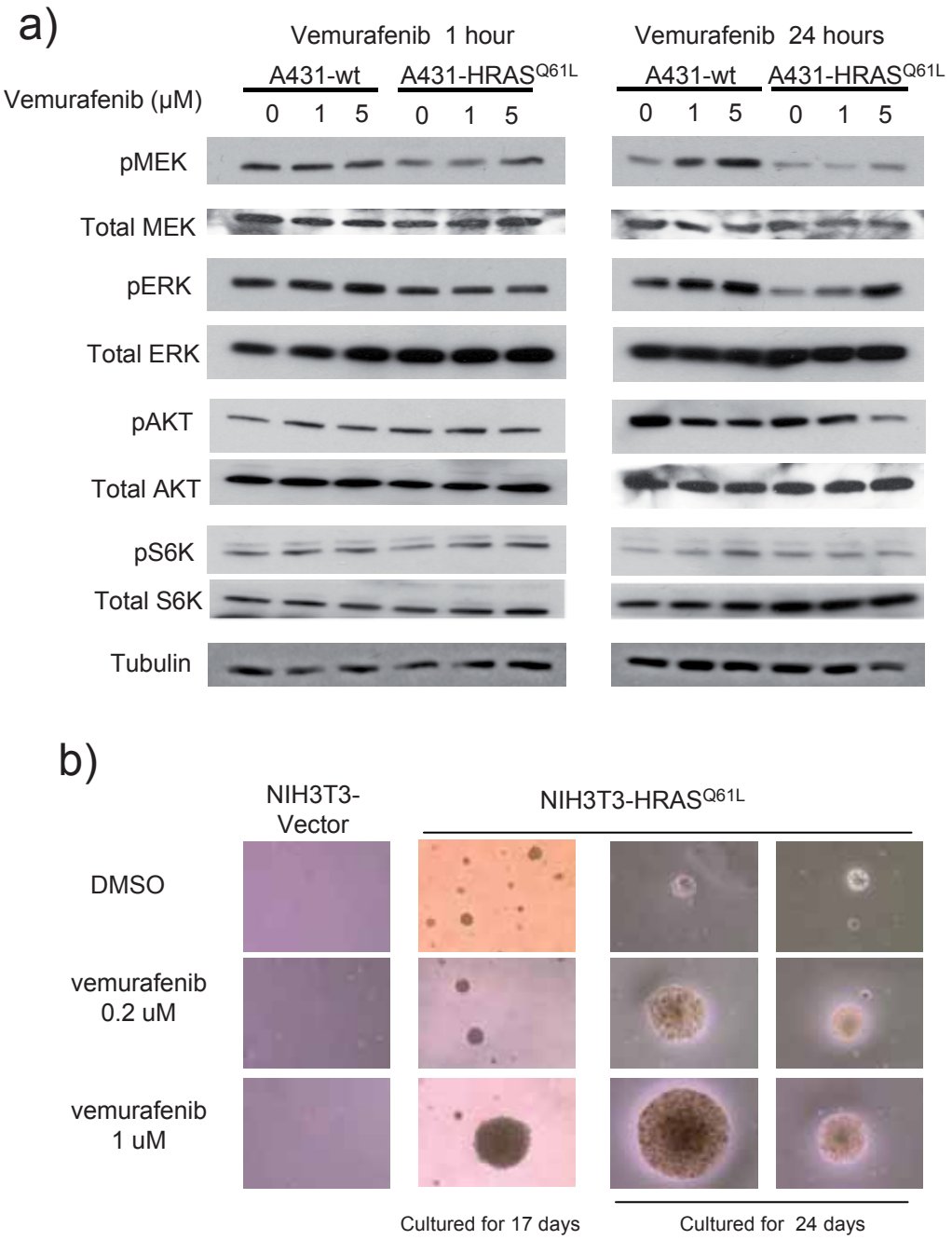

A

Papilloma

KA/SCC

Invasion

DMBA/
TPA

DMBA/
TPA/
PLX

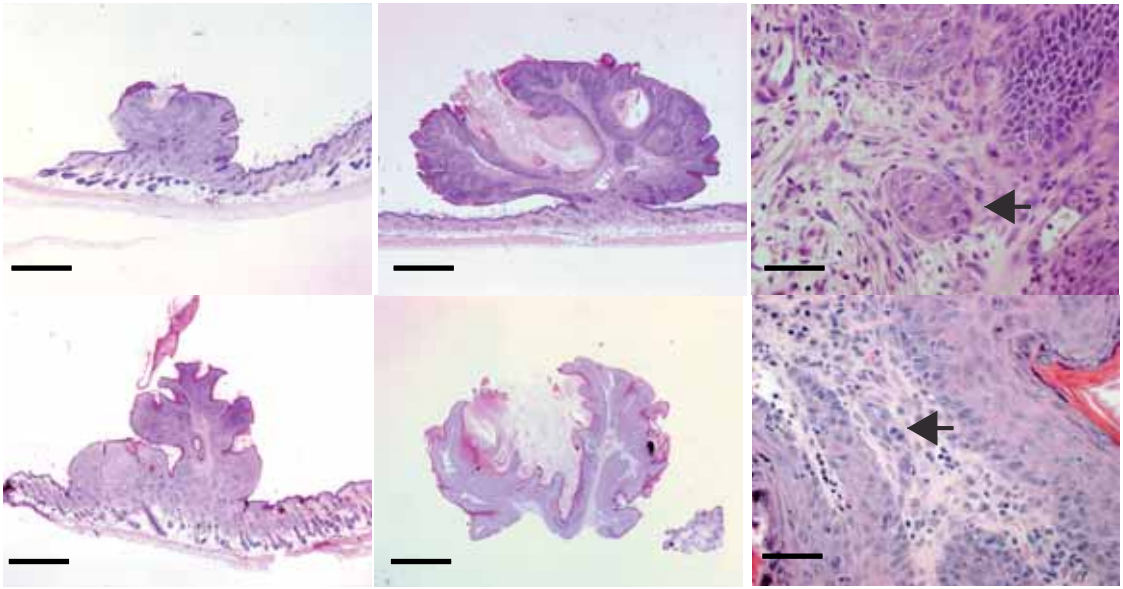

B

DMBA/TPA

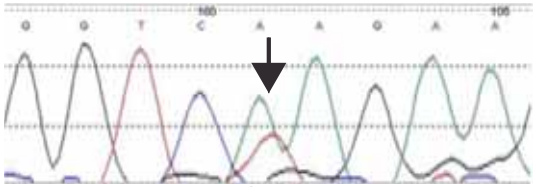

CTA
Q61L *Hras*

DMBA/TPA/PLX

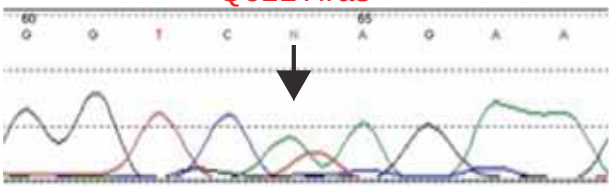

CTA
Q61L *Hras*

Supplemental Figure 7

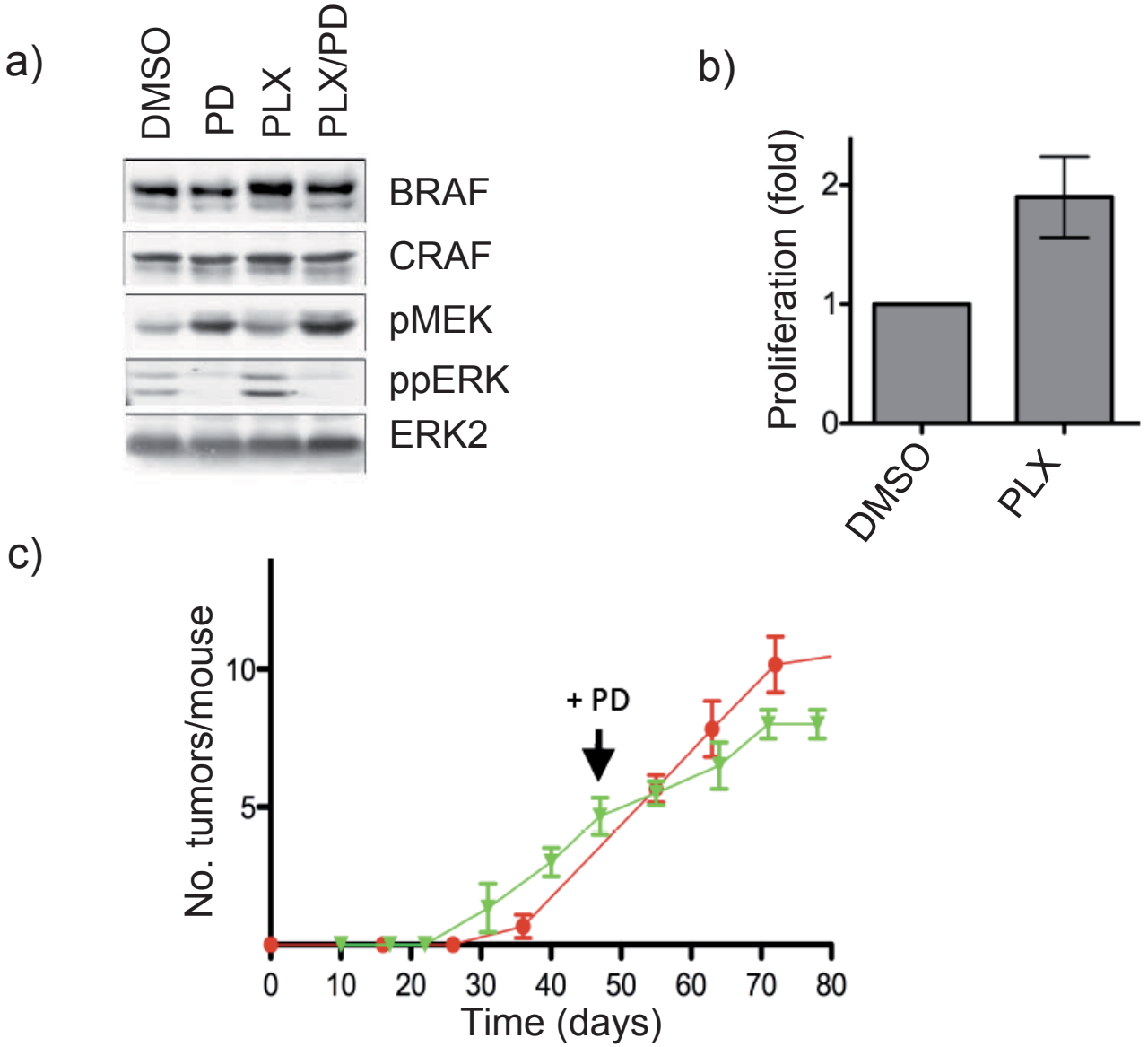

Topical 5-Fluorouracil Elicits Regressions of BRAF Inhibitor–Induced Cutaneous Squamous Cell Carcinoma

Journal of Investigative Dermatology advance online publication, 16 August 2012; doi:10.1038/jid.2012.268

TO THE EDITOR

The protein kinase BRAF regulates cell growth through the mitogen-activated protein kinase (MAPK) pathway. In about half of the melanomas, BRAF is mutated and acts as a driver oncogene that stimulates cell proliferation, survival, and tumor progression (Davies *et al.*, 2002; Gray-Schopfer *et al.*, 2007). The anti-BRAF drugs vemurafenib (PLX4032/RG7204) and dabrafenib (GSK2118436) achieve objective clinical responses in about 60% of melanoma patients whose tumors express mutant BRAF (Flaherty *et al.*, 2010; Chapman *et al.*, 2011; Sosman *et al.*, 2012), validating these drugs as a therapeutic option for BRAF-mutant melanoma patients.

An unexpected side effect of vemurafenib is that it induces keratoacanthomas (KA) and well-differentiated cutaneous squamous cell carcinomas (cuSCCs) in ~26% of patients (Flaherty *et al.*, 2010; Sosman *et al.*, 2012). This is because, although BRAF inhibitors block MAPK signaling in cells harboring BRAF mutations, they activate the pathway in cells expressing mutant RAS (Rat sarcoma) or when RAS is activated by receptor tyrosine kinases (Hatzivassiliou *et al.*, 2010; Heidorn *et al.*, 2010; Poulikakos *et al.*, 2010). Critically, 21–57% of the nonmelanoma skin lesions that develop in vemurafenib-treated patients carry somatic mutations in *HRAS* or *KRAS* (Oberholzer *et al.*, 2011; Su *et al.*, 2012).

We recently used a mouse two-stage skin carcinogenesis model to investigate how BRAF inhibitors drive the development of these nonmelanoma skin lesions (Su *et al.*, 2012). FVB/N mice were treated with a single topical application of the carcinogen 7,

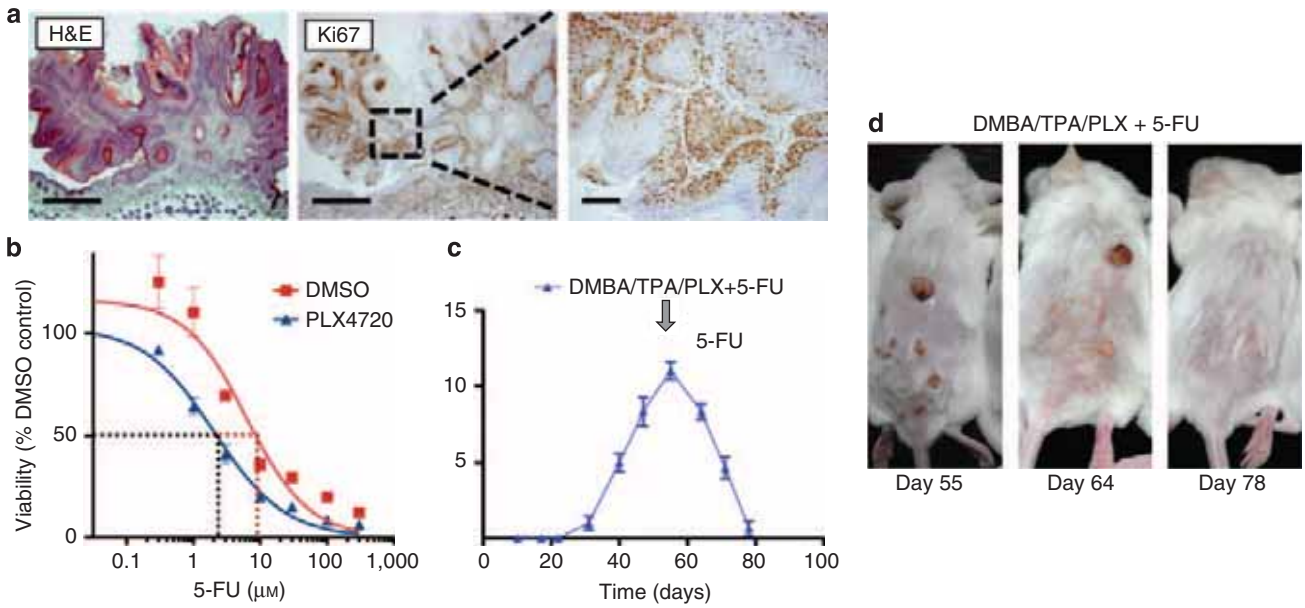

Figure 1. 5-Fluorouracil (5-FU) induces regression of the highly proliferative PLX4072-induced lesions in mice. (**a**) Photomicrographs showing hematoxylin and eosin (H&E) staining and high proliferation index in a Ki-67 immunohistochemical staining for a papilloma from a 7,12-dimethylbenz-(a)anthracene (DMBA)-, 12-O-tetradecanoyl-phorbol-13-acetate (TPA)-, and PLX4720-treated animal. Proliferation is more pronounced in the lower two-thirds of the epidermis. (**b**) Dose–response curves comparing RAS-transformed keratinocytes treated with 5-FU in the presence or absence of PLX4720. (**c**) Tumor development in DMBA-, TPA-, and PLX4720-treated mice (DMBA/TPA/PLX). Mice were treated with 5-FU on day 55 (indicated by the gray arrow) applied topically directly to single lesions twice a week. (**d**) Photographs show a single mouse from the 5-FU-treated cohort at days 55, 64, and 78. Bar = 0.5 mm left and center, 200 μm right.

Abbreviations: CuSCCs, cutaneous squamous cell carcinomas; DMBA, 7,12-dimethylbenz-(a)anthracene; KA, keratoacanthomas; MAPK, mitogen-activated protein kinase; TPA, 12-O-tetradecanoyl-phorbol-13-acetate; 5-FU, 5-fluorouracil

12-dimethylbenz-(a)anthracene (DMBA), which induces HRAS Q61L mutations in keratinocytes. The mice were then treated weekly with the tumor promoter 12-O-tetradecanoyl-phorbol-13-acetate (TPA) and daily with oral doses of PLX4270 (see Supplementary Experimental Procedures online), a BRAF inhibitor that is preferred for mouse studies because of its superior oral bioavailability (Su *et al.*, 2012). We demonstrated that PLX4720 accelerated the growth of squamoproliferative lesions in DMBA/TPA-treated mice but did not induce lesions in mice treated with DMBA alone (Su *et al.*, 2012). These data demonstrated that vemurafenib is not a tumor promoter *per se*; rather, it acts by accelerating the progression of preexisting, premalignant lesions in susceptible individuals.

It is not known whether the cuSCCs that develop in vemurafenib-treated patients have metastatic potential different from cuSCCs that develop in the absence of BRAF inhibition, because in both the clinical settings these lesions are treated by surgical excision. However, advanced-stage melanoma patients on BRAF inhibitors can develop multiple eruptive lesions early during the course of BRAF inhibitor therapy and these can be challenging to manage surgically. We therefore sought to develop a noninvasive approach to treat these particular patients.

Previous studies have shown that BRAF inhibitors accelerate the proliferation of RAS-transformed cells (Hatzivassiliou *et al.*, 2010; Heidorn *et al.*, 2010; Poulikakos *et al.*, 2010; Su *et al.*, 2012). We confirmed that the nonmelanoma skin lesions in DMBA/TPA/PLX4720-treated mice have a high proliferative index by showing that they have a high mitotic index (5 × 10 high-power fields) and strong positive staining for Ki-67 (Figure 1a), and thus we

Figure 2. 5-Fluorouracil (5-FU) induces regression of BRAF inhibitor–induced squamoproliferative lesions in patients. (**a**) Eruptive actinic keratosis and nascent cutaneous squamous cell carcinomas (cuSCCs) on day 9 of dabrafenib therapy in patient #1. Black arrows point at cuSCCs, white arrow points at clinically diagnosed keratoacanthoma. (**b**) In patient #1, lesions consistent with a clinical diagnosis of cuSCC were either treated with 5-FU twice daily (equivalent sites numbered in red and blue arrows) or left untreated (numbered in black) for 28 days, beginning from day 12 of dabrafenib therapy. Lesion marked #1 is a presumptive seborrheic keratosis, serving as a positional and size reference. (**c**) In patient #2, who was also treated with dabrafenib against melanoma, two keratotic cuSCCs were treated simultaneously with twice daily 5-FU applications. Photographs were taken on days 0, 17, 34, and 62 of treatment.

investigated whether antiproliferative drugs could induce their regression.

5-Fluorouracil (5-FU) is an antimetabolite that blocks DNA synthesis and inhibits cell proliferation. Although topical application of 5-FU should be restricted to an area no greater than 500 cm^2 (approximately the area of an extended hand) (MedaPharmaceuticals, 2012), 5-FU is inexpensive and achieves objective clinical responses in 46–87% of cases of solar keratosis, lesions that are the precursor of invasive cuSCC (Gray and Meland, 2000; Shimizu *et al.*, 2011). We confirm that 5-FU inhibited the growth of PDV cells, an HRAS mutant keratinocyte line, with IC_{50} (half maximal inhibitory concentration 50) values of ~4.43 μM in the absence of PLX4720 and ~1.67 μM in its presence (Figure 1b). To test 5-FU *in vivo*, FVB/N mice (six animals per group) were treated with DMBA, TPA, and PLX4720 as described (Su *et al.*, 2012). As reported (Su *et al.*, 2012), palpable lesions first appeared after 30 days, increasing in number to approximately 11 lesions per mouse in 55 days (Figure 1c). We then treated the individual lesions with topical 5% 5-FU cream twice a week. Left untreated, we have shown that the tumors continue to grow and reach tumor burden limits after approximately 90 days (Su *et al.*, 2012); however, with 5-FU, we observed an immediate response, with tumor regression leading to complete remission within 25 days (Figure 1c and d).

On the basis of these observations, we tested the efficacy of 5-FU in two melanoma patients who were being treated with the BRAF inhibitor dabrafenib (GSK2118436). Both patients rapidly developed multiple eruptive lesions consistent with actinic keratosis and/or cuSCC (Figure 2a and b). Individual lesions were treated with 5% 5-FU cream twice a day, respecting recommended safety guidelines for total skin treatment area. Photo-documented lesions presenting the characteristics of KA and cuSCCs at various stages responded to 5-FU, whereas untreated concurrent lesions progressed and after biopsy were confirmed to be bona fide cuSCCs (Figure 2b and c). During follow-up periods of 11 and 18 months, respectively, none of the treated lesions in patients 1 and 2 recurred. As noted in these anecdotal cases, nascent lesions tended to respond more quickly compared with the established hyperkeratotic lesions.

Secondary malignancies induced by conventional chemotherapies generally take many years to develop (Curtis *et al.*, 1992), but the nonmelanoma skin lesions induced by BRAF inhibitors develop within weeks of initiating treatment (Su *et al.*, 2012). Our previous studies show that BRAF inhibitors are not carcinogens *per se*; rather, they act to accelerate the development of preexisting subclinical lesions in susceptible patients. The approval of vemurafenib raises a pressing clinical need to provide treatment guidelines to manage these secondary lesions in patients for whom surgery is an undesirable option. The observation that BRAF inhibitors drive proliferation of RAS-mutant keratinocytes led us to test the efficacy of antiproliferative agents. We show that 5-FU provides a safe, noninvasive, inexpensive, and effective alternative to surgical intervention in clinical cases in which multiple surgeries are difficult or in cases in which lesions are incipient.

Details concerning the ethics of animal and human studies are provided in the Supplementary Materials online.

CONFLICT OF INTEREST

The authors state no conflict of interest.

ACKNOWLEDGMENTS

We thank Mr Eric Ward, Dr Kay Savage (ICR), and Ms Annette Lane (ICR) for their technical assistance with immunohistochemical preparations.

Amaya Viros[1,2], Robert Hayward[1], Matthew Martin[1], Sharona Yashar[3], Clarissa C. Yu[4], Berta Sanchez-Laorden[1], Alfonso Zambon[5], Dan Niculescu-Duvaz[5], Caroline Springer[5], Roger S. Lo[4] and Richard Marais[1,6]

[1]Signal Transduction Team, The Institute of Cancer Research, London, UK; [2]Seccio Dermatologia, Departament de Medicina, Hospital Universitari Vall d'Hebron, Barcelona, Spain; [3]Department of Pathology and Laboratory Medicine, David Geffen School of Medicine, University of California, Los Angeles, Los Angeles, California, USA; [4]Division of Dermatology, Department of Medicine, David Geffen School of Medicine, University of California, Los Angeles, Los Angeles, California, USA; [5]Gene and Oncogene Targeting Team, CR-UK Cancer Therapeutics Unit, The Institute of Cancer Research, Sutton, Surrey, UK and [6]Molecular Oncology Laboratory, The Paterson Institute for Cancer Research, Manchester, UK
E-mail: rmarais@picr.man.ac.uk

SUPPLEMENTARY MATERIAL

Supplementary material is linked to the online version of the paper at http://www.nature.com/jid

REFERENCES

Chapman PB, Hauschild A, Robert C *et al.* (2011) Improved survival with vemurafenib in melanoma with BRAF V600E mutation. *N Engl J Med* 364:2507–16

Curtis RE, Boice Jr JD, Stovall M *et al.* (1992) Risk of leukemia after chemotherapy and radiation treatment for breast cancer. *N Engl J Med* 326:1745–51

Davies H, Bignell GR, Cox C *et al.* (2002) Mutations of the BRAF gene in human cancer. *Nature* 417:949–54

Flaherty KT, Puzanov I, Kim KB *et al.* (2010) Inhibition of mutated, activated BRAF in metastatic melanoma. *N Engl J Med* 363: 809–19

Gray RJ, Meland NB (2000) Topical 5-fluorouracil as primary therapy for keratoacanthoma. *Ann Plast Surg* 44:82–5

Gray-Schopfer V, Wellbrock C, Marais R (2007) Melanoma biology and new targeted therapy. *Nature* 445:851–7

Hatzivassiliou G, Song K, Yen I *et al.* (2010) RAF inhibitors prime wild-type RAF to activate the MAPK pathway and enhance growth. *Nature* 464:431–5

Heidorn SJ, Milagre C, Whittaker S *et al.* (2010) Kinase-dead BRAF and oncogenic RAS cooperate to drive tumor progression through CRAF. *Cell* 140:209–21

MedaPharmaceuticals (2012) *Summary of Product Characteristics* http://www.medicines.org.uk/EMC/medicine/6219/SPC/Efudix+Cream/

Oberholzer PA, Kee D, Dziunycz P. *et al.* (2011) RAS mutations are associated with the development of cutaneous squamous cell tumors in patients treated with RAF inhibitors. *J Clin Oncol* 30:316–21

Poulikakos PI, Zhang C, Bollag G *et al.* (2010) RAF inhibitors transactivate RAF dimers and ERK signalling in cells with wild-type BRAF. *Nature* 464:427–30

Shimizu I, Cruz A, Chang KH *et al.* (2011) Treatment of squamous cell carcinoma *in situ*: a review. *Dermatol Surg* 37:1394–411

Sosman JA, Kim KB, Schuchter L *et al.* (2012) Survival in BRAF V600-mutant advanced melanoma treated with vemurafenib. *N Engl J Med* 366:707–14

Su F, Viros A, Milagre C *et al.* (2012) RAS mutations in cutaneous squamous-cell carcinomas in patients treated with BRAF inhibitors. *N Engl J Med* 366:207–15

SUPPLEMENTARY EXPERIMENTAL PROCEDURES

Animal procedures were performed following National Home Office regulations under the Animals (Scientific Procedures) Act 1986, with ethical approval from the Institute of Cancer Research Animal Ethics Committee; with the guidance of the Committee of the National Cancer Research Institute. We used a two-stage skin carcinogenesis model in FVB/N mice, treating the shaved backs with a single dose of the carcinogen DMBA (100μg), followed by weekly applications of the pro-inflammatory agent TPA (5μg) with six animals per group. PLX4720 was delivered by oral gavage (25mg/kg/day) throughout the 80 day experiment. We used bi-weekly topical application of 5-FU for treatment of mouse lesions.

The patients provided written informed consent and were enrolled in a clinical trial study of dabrafenib in patients with $BRAF^{V600E}$-driven metastatic melanoma approved by the research ethics committee of UCLA. Patients applied 5-FU twice daily.

Topical 5-Fluorouracil Elicits Regressions of BRAF Inhibitor–Induced Cutaneous Squamous Cell Carcinoma

Amaya Viros, Robert Hayward, Matthew Martin, Sharona Yashar, Clarissa C. Yu, Berta Sanchez-Laorden, Alfonso Zambon, Dan Niculescu-Duvaz, Caroline Springer, Roger S. Lo and Richard Marais

Journal of Investigative Dermatology (2013) **0,** 000–000. doi:10.1038/jid.2013.12

Correction to: *Journal of Investigative Dermatology* (2013) **133**, 274–276; doi:10.1038/jid.2012.268; published online 16 August 2012

Following the publication of this article, the authors noted that the second affiliation for Dr Amaya Viros is incomplete. The work was performed at Seccio Dermatologia, Departament de Medicina, Hospital Universitari Vall d'Hebron, Universitat Autonoma de Barcelona, Spain. The authors regret the error.